factors of the pancreas [8, 14, 15]. The deletion of the notochord in cultured chick embryos results in the loss of the dorsal pancreatic gene expression. Moreover, the co-culture of the notochord with the endoderm fates to become pancreas restoring the expression of pancreatic genes. This important observation clarified the role of the focal sonic hedgehog (shh) inhibition and regulation of Pancreas-duodenum homeobox 1 (pdx-1) by activin and FGF-2 along the fore/midgut, thus resulting in three different derived tissues, namely stomach (shh-positive, pdx-1-negative), pancreas (shh-negative, pdx-1-positive), and duodenum (shh-positive, pdx-1-positive) (Fig. **2**) [8]. These results indicate the key role of the anatomically related tissues in the proper pancreatic development. The dominant and localized expression of pdx-1 and hlxb9 (homeobox transcription factor), while shh is repressed along the fore/midgut derived tissues, is one of the main characteristics of the primitive pancreas [8, 12, 14, 16].

PANCREATIC ENDOCRINE CELL-FATE DIFFERENTIATION

Although, most of the stimulation of the primitive pancreas is mainly directed toward its dorsal part, it has also a great influence over the ventral segment. Particularly, the common pancreatic phenotype (pdx-1+, hlxb9+ and shh-) will be equally adopted after both the dorsal and ventral parts merge [8, 12]. Briefly, a new transitional change may take place, which will initiate the derivation of the two cell populations later recognized in the adult tissues as the endocrine- and exocrine-derived cells. The regulation of the cell-fate differentiation process involves the expression of the several of the well-coordinated transcriptional factors and signals, known as the Delta-Notch signaling system (Fig. **3**) [12, 16-18]. Both exocrine and endocrine may transiently retain, at least in part, the common pancreatic phenotype, but then differentiate and commit to the exocrine progenitor expressing both the pancreas specific transcription factor 1a (Ptf1a-p48) and the hairy and enhancer of the split homolog (Hes1). Hes1 is actually a transient repressor which allows the exocrine cell progenitors to proliferate partially undifferentiated, while their progeny will only express Ptf1a-p48 [12, 17, 18]. In contrast, the early endocrine progenitors will express initially Ngn-3 and later co-express Beta2/Neuro D and others upon commitment to each specific-endocrine lineage. *In vivo* endocrine cell-fate differentiation occurs in a very peculiar manner. Within the primitive acinar aggregates, only the central cells became Ngn-3 expressing endocrine progenitors. Those Ngn-3 expressing endocrine progenitors will eventually be surrounded by exocrine cell progenitors in a process called lateral inhibition. Several parts of this lateral inhibition process remain unknown, but new evidence points to the key roles that the mesenchyma and the extracellular matrices play in the process, such as growth differentiation factor 11 (GDF11) and laminin-1 (Fig. **3**) [19-24]. The capacity of further proliferation of such progenitor cells is mainly driven by fibroblast growth factors (FGFs) [25-27]. The surrounding mesenchyme regulates the timing and growth factors for the proper pancreatic development in both the exocrine and endocrine cell progenitors [28]. The expression of Isl-1 within the mesenchyme of the primitive pancreas regulates the transitional differentiation of the primitive pancreatic epithelium to the endocrine cells, increasing the endocrine population [29]. Moreover, the endocrine cell population can also be enriched from a subset of hepatocyte nuclear factor 1-β (HNF1β) expressing cells, which transiently express Ngn-3 [30, 31]. The Ngn-3 expressing cells can rapidly proliferate as common endocrine progenitors, while differentiated α-, β-, and δ-cells cannot, once they commit to their final lineage during the development of the pancreas [18, 21, 32]. Later, during the terminal fetal growth [18, 21] and the postnatal period, the differentiated endocrine cells are able to reenter into the cell cycle [33, 34]. It is clear that the Ngn-3 positive cells play a major role in the embryonic development of the pancreas, giving rise to the whole pancreatic endocrine lineages. Nevertheless, their contribution to the balance of adult tissue remains unclear. Recent evidence has indicated that their population dramatically declines at birth and becomes undetectable in adult tissues even during pancreatic regeneration after surgical injury [20, 35].

ENDOCRINE LINEAGE SPECIFIC-DIFFERENTIATIONAND MATURATION

The development of the pancreas requires the orchestration of several specific transcriptional and growth factors. Many studies have been conducted to determine the interactions between the pancreatic epithelium and the mesenchyma to terminally differentiate the hormone-secreting cells [18, 29, 36]. Some investigators have reported that glucagon is the first

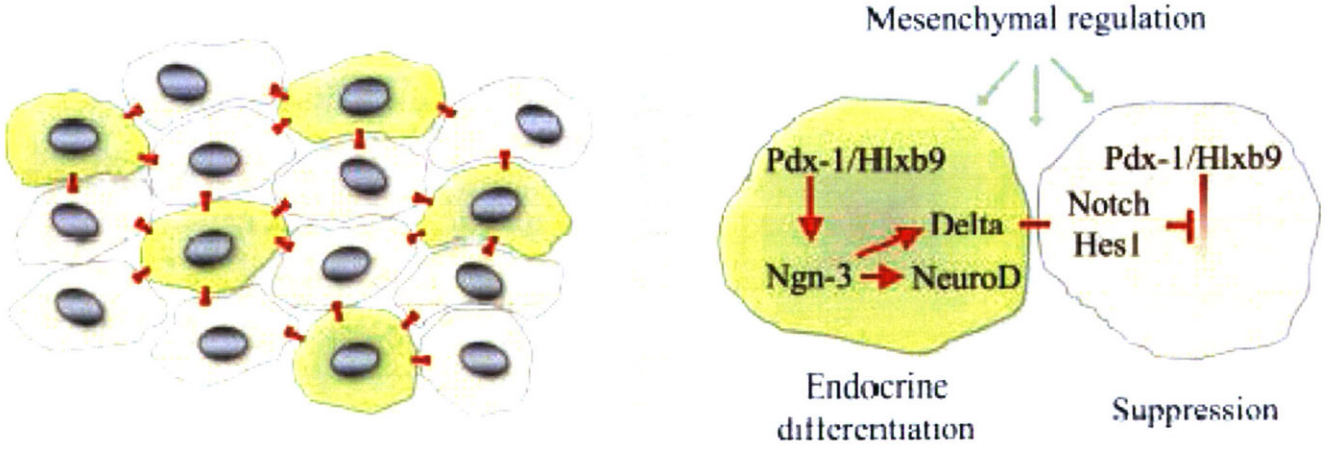

Fig. (3). Endocrine cell-fate differentiation of the developing pancreas.

A schematic draw shows the regulation of the cell-fate differentiation of the early pancreas-committed stem cells (pdx-1+, hlxb9+ and shh-) into endocrine precursors (Ngn3+) by cell-cell Delta-Notch signaling while the neighbor cells are repressed (pdx-1+, Hes1+, and Ngn3-) by a process called lateral inhibition.

peptide hormone to be detected in the developing pancreas [36, 37].

The use of antisense oligonucleotides against preproglucagon in the developing pancreas on E11-13 grown in tissue culture resulted in the marked inhibition of insulin gene expression. In contrast, a developing pancreas on E15 grown under the same conditions without antisense showed a normal level and pattern of insulin gene expression [36]. These observations strongly suggest the interactions of the early-differentiated glucagon-expressing cells on the terminal differentiation of the β-cells. Despite the co-existence of both α- and β-cells in the adult pancreas, the cells have antagonistic roles against each other. Both α- and β-cells are derived from a common progenitor, Ngn3-expressing cells, during the development of the pancreas. β-cells express insulin and MafA at a 250-fold higher rate than α-cells. In contrast, α-cells expressed glucagon and MafB at a 450-fold higher rate than β-cells. In addition, researchers have found new evidence that the expression of MafB precedes that of MafA during β-cell differentiation in the pancreas and that the differential expression of NK6 transcription factor related locus 1 (Nkx6.1) in MafB+ cells defines whether the cells express insulin or glucagon. The appearance of Nkx6.1 expression and the increased expression of pdx-1 is critical for the terminal differentiation of β-cells at this last stage. Particularly, at this point the co-expression of Nkx6.1 with the high re-expression of pdx-1 drives the insulin gene expression in the young β-cells. The expression of MafA is involved in the process of both fetal and post-natal β-cell replication and maturation (Fig. **4**) [38]. The loss of MafA expression maintains the normal pancreatic morphology at birth, but after birth it reduces the proportion of β-cells with an impaired glucose tolerance and the occurrence of diabetes [39]. The β-cells derived from the adult pancreas have a glucose-induced insulin secretion and a comparatively higher amount of insulin secretion, whereas the fetal and neonatal islets are not yet glucose-responsiveness [38]. Both the fetal and neonatal insulin-expressing cells achieve glucose-responsiveness after they show the high expression of glucose transporter 2 (Glut2). However, Glut2 is expressed either in MafA+, Nkx6.1+, and pdx-1+ (young β-cells), or MafB+, Nkx6.1+, or pdx-1+ cells (fetal β-cells). This observation suggests that the switch from MafB to MafA may not be necessary in order to initiate the Glut2 expression but it meaningfully contributes to the β-cell replication and maturation [38]. Therefore, the low Glut2 expression may be considered as a cell marker of the β-cell specific precursors rather than the mature β-cells. After birth, the rapid proliferation of β-cells is mainly driven by cyclin D2 and Ki67 and β-cells improve their capacity to secrete insulin in order to properly control the increasing metabolic demands [33, 34].

CURRENT STATUS OF DIFFERENTIATION OF HUMAN ES CELLS TO ISLET-LIKE CELLS

Assady et. al. utilized EB formation as a platform to generate insulin-secreting cells in human ES cells in 2001[40]. In 2005, Brolen *et al.* performed a co-transplantation of a mouse developing pancreas, which could provide the signaling necessary to facilitate the differentiation of human ES cells to insulin-secreting cells *in vivo* [41]. In 2006, Xu *et al.* reported the derivation of the pancreatic endoderm lineage using three different types of inducing methods: 1) EB formation, 2) spontaneous differentiation, and 3) definitive endodermal induction [42]. Recently, D'Amour *et al.* reported an interesting

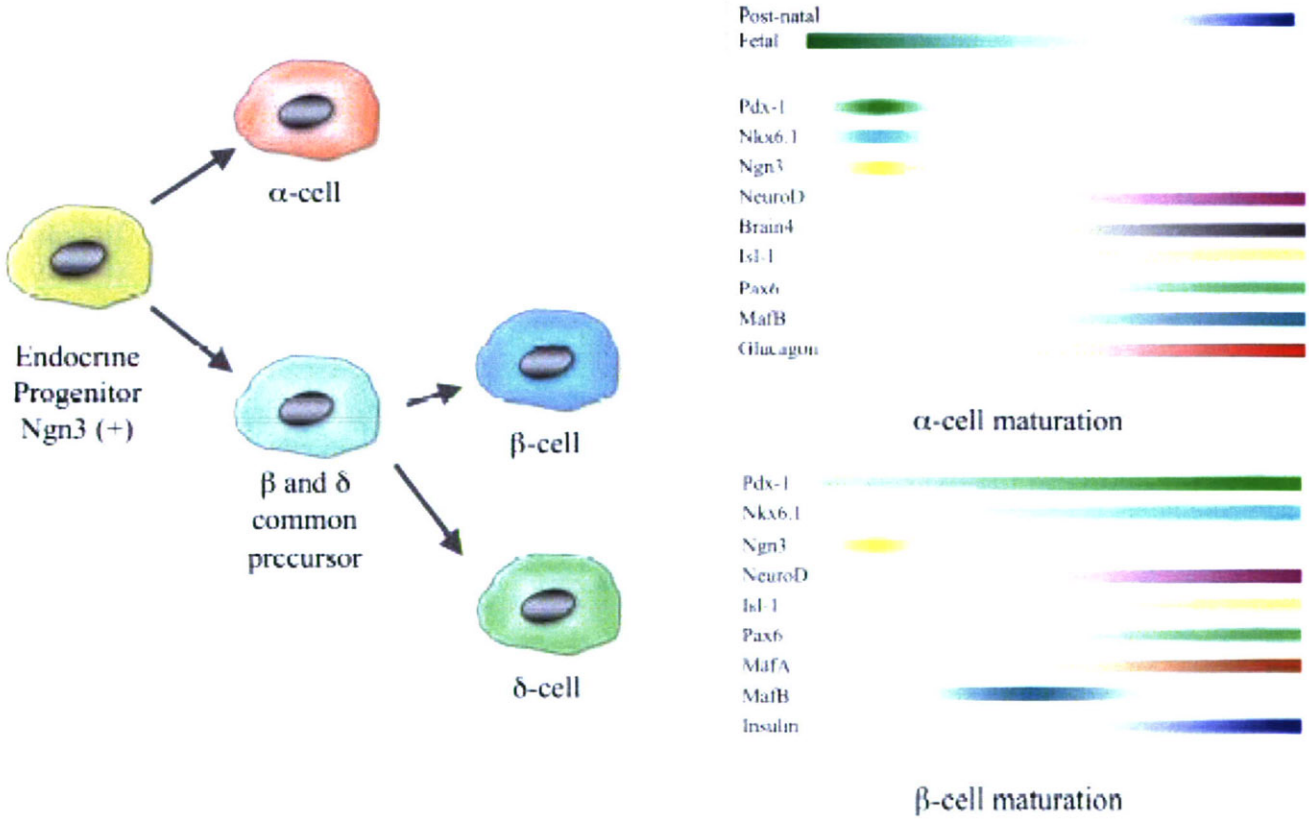

Fig. (4). Terminal differentiation and maturation of the endocrine pancreatic-lineages.

The *left panel* shows the terminal endocrine differentiation of the islet derived from its common progenitor (Ngn3+). The *right panel* illustrates the timing and expression of the transcriptional factors during the α- and β-cell maturation.

protocol in human ES cells, which allows for the *in vitro* derivation of the cells existing in the posterior foregut from the definitive endoderm committed cells using cyclopamine, retinoic acid (RA) and fibroblast growth factor-10 (FGF-10) [43]. Cyclopamine is well recognized as one of the most potent shh inhibitors, but it also exhibits a teratogenic adverse effect [44]. This protocol generates pancreatic islet-like cells capable of expressing the main hormones insulin, glucagon, and somatostatin. However, the lack of controlled generation of the endocrine progenitor, Ngn-3-expressing cells, in their protocol have limited the large production of pancreatic endocrine cells. Moreover, the finally generated, ES-derived β-cells retain a fetal phenotype by expressing only MafB and not MafA, and thus lack a glucose-sensitive insulin secreting capacity [43]. The next step should be to address how to generate Ngn-3-expressing cells *in vitro* for the large production of pancreatic endocrine cells, and then to explore a method to maturate such cells to β-cells with an adult phenotype.

CONCLUSIONS AND FUTURE PERSPECTIVES

The insulin-producing cells generated from ES cells represent an attractive alternative source to the cadaveric isolated pancreatic islets for the treatment of diabetes. However, the efficient differentiation of ES cells into β–like-cells still remains a big challenge. The lack of success in the early attempts has revealed the importance of a better understanding of the fundamental normal development of the pancreas.

Considering that the pancreas is exclusively derived from the definitive endoderm and that the endocrine cell population represents a minority, a successful β-cell differentiation would require a high definitive endoderm commitment rather than a visceral endoderm, or ectoderm, which arises from aberrant differentiated cells with a most likely incomplete expression of the β-cell markers and lack of function [45].

Of course, the screening of cytokines and growth factors and the invention of new synthetic biochemicals will both be required in order to selectively control the differentiation and proliferation of stem cells.

Ultimately, such newly developed chemical compounds may provide new insights into stem cells and our understanding of the mechanisms that drive tissue regeneration and homeostasis.

ACKNOWLEDGMENT

This work was supported in part by a Grant-in-Aid for Scientific Research (B) from the Japan Society for the Promotion of Science (JSPS) to N.K.

ABBREVIATIONS

ES	=	embryonic stem cells
EB	=	embryoid bodies
ITS	=	insulin-transferrin-sodium selenium
EGF	=	epithelial growth factor
FGF-2	=	fibroblast growth factor-2
PS	=	primitive streak
GSC	=	goosecoid
Foxa2	=	forkhead box A2
CXCR-4	=	chemokine C-X-C motif receptor 4
Sox17α/β	=	sex determining region-Y box 17
VEGFR2	=	vascular endothelial growth factor receptor-2
PDGFRα	=	platelet-derived growth factor receptor-α
GATA-4	=	GATA binding protein 4
AFP	=	α-fetoprotein
Ngn3	=	neurogenin-3
Isl-1	=	islet-1
Shh	=	sonic hedgehog
Pdx1	=	pancreas-duodenum homeobox 1
Hlxb9	=	homeobox transcription factor
Ptf1a-p48	=	pancreas specific transcription factor 1a
Hes1	=	hairy and enhancer of split homolog
GDF11	=	growth differentiation factor 11
FGF	=	fibroblast growth factors
HNF1β	=	hepatocyte nuclear factor 1 β
Nkx6.1	=	NK6 transcription factor related locus 1
and Glut2	=	glucose transporter 2

REFERENCES

[1] Ryan, E. A.; Lakey, J. R.; Rajotte, R. V.; Korbutt, G. S.; Kin, T.; Imes, S.; Rabinovitch, A.; Elliott, J. F.; Bigam, D.; Kneteman, N. M.; Warnock, G. L.; Larsen, I.; Shapiro, A. M. *Diabetes* **2001**, *50*, 710.
[2] Shapiro, A. M.; Lakey, J. R.; Ryan, E. A.; Korbutt, G. S.; Toth, E.; Warnock, G. L.; Kneteman, N. M.; Rajotte, R. V. *N. Eng. J. Med.* **2000**, *343*, 230.
[3] Thomson, J. A.; Itskovitz-Eldor, J.; Shapiro, S. S.; Waknitz, M. A.; Swiergiel, J. J.; Marshall, V. S.; Jones, J. M. *Science* **1998**, *282*, 1145.
[4] Kania, G.; Blyszczuk, P.; Wobus, A. M. *Int. J. Dev. Biol.* **2004**, *48*, 1061.
[5] Lumelsky, N.; Blondel, O.; Laeng, P.; Velasco, I.; Ravin, R.; McKay, R. *Science* **2001**, *292*, 1389.
[6] Rajagopal, J.; Anderson, W. J.; Kume, S.; Martinez, O. I.; Melton, D. A. *Science* **2003**, *299*, 363.
[7] Sipione, S.; Eshpeter, A.; Lyon, J. G.; Korbutt, G. S.; Bleackley, R. C. *Diabetologia* **2004**, *47*, 499.
[8] Wells, J. M.; Melton, D. A. *Annu. Rev. Cell Dev. Biol.* **1999**, *15*, 393.
[9] Yasunaga, M.; Tada, S.; Torikai-Nishikawa, S.; Nakano, Y.; Okada, M.; Jakt, L. M.; Nishikawa, S.; Chiba, T.; Era, T.; Nishikawa, S. *Nat. Biotechnol.* **2005**, *23*, 1542.
[10] Giddings, S. J.; King, C. D.; Harman, K. W.; Flood, J. F.; Carnaghi, L. R. *Nat. Genet.* **1994**, *6*, 310.
[11] Ku, H. T.; Zhang, N.; Kubo, A.; O'Connor, R.; Mao, M.; Keller, G.; Bromberg, J. S. *Stem Cells* **2004**, *22*, 1205.
[12] Edlund, H. *Diabetes* **2001**, *50* (Suppl 1), S5.
[13] D'Amour, K. A.; Agulnick, A. D.; Eliazer, S.; Kelly, O. G.; Kroon, E.; Baetge, E. E. *Nat. Biotechnol.* **2005**, *23*, 1534.
[14] Soria, B. *Differentiation* **2001**, *68*, 205.
[15] Wells, J. M.; Melton, D. A. *Development* **2000**, *127*, 1563.
[16] Edlund, H. *Diabetes* **1998**, *47*, 1817.
[17] Apelqvist, A.; Li, H.; Sommer, L.; Beatus, P.; Anderson, D. J.; Honjo, T.; Hrabe de Angelis, M.; Lendahl, U.; Edlund, H. *Nature* **1999**, *400*, 877.
[18] Jensen, J. *Dev. Dyn.* **2004**, *229*, 176.
[19] Dichmann, D. S.; Yassin, H.; Serup, P. *Dev. Dyn.* **2006**, *235*, 3016.
[20] Harmon, E. B.; Apelqvist, A. A.; Smart, N. G.; Gu, X.; Osborne, D. H.; Kim, S. K. *Development* **2004**, *131*, 6163.
[21] Jiang, F. X.; Cram, D. S.; DeAizpurua, H. J.; Harrison, L. C. *Diabetes* **1999**, *48*, 722.
[22] Jiang, F. X.; Georges-Labouesse, E.; Harrison, L. C. *Mol. Med.* **2001**, *7*, 107.
[23] Jiang, F. X.; Harrison, L. C. *Exp. Cell Res.* **2005**, *308*, 114.
[24] Jiang, F. X.; Harrison, L. C. *Differentiation* **2005**, *73*, 45.
[25] Cras-Meneur, C.; Elghazi, L.; Czernichow, P.; Scharfmann, R. *Diabetes* **2001**, *50*, 1571.
[26] Elghazi, L.; Cras-Meneur, C.; Czernichow, P.; Scharfmann, R. *Proc. Natl. Acad. Sci. USA* **2002**, *99*, 3884.
[27] Hart, A.; Papadopoulou, S.; Edlund, H. *Dev. Dyn.* **2003**, *228*, 185.
[28] Scharfmann, R. *Diabetologia* **2000**, *43*, 1083.
[29] Ahlgren, U.; Pfaff, S. L.; Jessell, T. M.; Edlund, T.; Edlund, H. *Nature* **1997**, *385*, 257.
[30] Gu, G.; Dubauskaite, J.; Melton, D. A. *Development* **2002**, *129*, 2447.
[31] Gu, G.; Wells, J. M.; Dombkowski, D.; Preffer, F.; Aronow, B.; Melton, D. A. *Development* **2004**, *131*, 165.
[32] Jensen, J.; Heller, R. S.; Funder-Nielsen, T.; Pedersen, E. E.; Lindsell, C.; Weinmaster, G.; Madsen, O. D.; Serup, P. *Diabetes* **2000**, *49*, 163.

[33] Dor, Y.; Brown, J.; Martinez, O. I.; Melton, D. A. *Nature* **2004**, *429*, 41.
[34] Georgia, S.; Bhushan, A. *J. Clin. Invest.* **2004**, *114*, 963-968.
[35] Lee, C. S.; De Leon, D. D.; Kaestner, K. H.; Stoffers, D. A. *Diabetes* **2006**, *55*, 269.
[36] Prasadan, K.; Daume, E.; Preuett, B.; Spilde, T.; Bhatia, A.; Kobayashi, H.; Hembree, M.; Manna, P.; Gittes, G. K. *Diabetes* **2002**, *51*, 3229.
[37] Rall, L. B.; Pictet, R. L.; Williams, R. H.; Rutter, W. J. *Proc. Natl. Acad. Sci. USA* **1973**, *70*, 3478.
[38] Nishimura, W.; Kondo, T.; Salameh, T.; El Khattabi, I.; Dodge, R.; Bonner-Weir, S.; Sharma, A. *Dev. Biol.* **2006**, *293*, 526.
[39] Zhang, C.; Moriguchi, T.; Kajihara, M.; Esaki, R.; Harada, A.; Shimohata, H.; Oishi, H.; Hamada, M.; Morito, N.; Hasegawa, K.; Kudo, T.; Engel, J. D.; Yamamoto, M.; Takahashi, S. *Mol. Cell Biol.* **2005**, *25*, 4969.
[40] Assady, S.; Maor, G.; Amit, M.; Itskovitz-Eldor, J.; Skorecki, K. L.; Tzukerman, M. *Diabetes* **2001**, *50*, 1691.
[41] Brolen, G. K.; Heins, N.; Edsbagge, J.; Semb, H. *Diabetes* **2005**, *54*, 2867.
[42] Xu, X.; Kahan, B.; Forgianni, A.; Jing, P.; Jacobson, L.; Browning, V.; Treff, N.; Odorico, J. *Cloning Stem Cells* **2006**, *8*, 96.
[43] D'Amour, K. A.; Bang, A. G.; Eliazer, S.; Kelly, O. G.; Agulnick, A. D.; Smart, N. G.; Moorman, M. A.; Kroon, E.; Carpenter, M. K.; Baetge, E. E. *Nat. Biotechnol.* **2006**, *24*, 1392.
[44] Cooper, M. K.; Porter, J. A.; Young, K. E.; Beachy, P. A. *Science* **1998**, *280*, 1603.
[45] Bonner-Weir, S.; Weir, G. C. *Nat. Biotechnol.* **2005**, *23*, 857.

Original Article

Cell-Permeable Pentapeptide V5 Inhibits Apoptosis and Enhances Insulin Secretion, Allowing Experimental Single-Donor Islet Transplantation in Mice

Jorge D. Rivas-Carrillo,[1] Alejandro Soto-Gutierrez,[1] Nalu Navarro-Alvarez,[1] Hirofumi Noguchi,[2] Teru Okitsu,[3] Yong Chen,[1] Takeshi Yuasa,[1] Kimiaki Tanaka,[1] Michiki Narushima,[1] Atsushi Miki,[1] Haruo Misawa,[4] Yasuhiko Tabata,[5] Hee-Sook Jun,[6,7] Shinichi Matsumoto,[8] Ira J. Fox,[9] Noriaki Tanaka,[1] and Naoya Kobayashi[1]

OBJECTIVE—Treatment of diabetic patients by pancreatic islet transplantation often requires the use of islets from two to four donors to produce insulin independence in a single recipient. Following isolation and transplantation, islets are susceptible to apoptosis, which limits their function and probably long-term islet graft survival.

RESEARCH DESIGN AND METHODS—To address this issue, we examined the effect of the cell-permeable apoptosis inhibitor pentapeptide Val-Pro-Met-Leu-Lys, V5, on pancreatic islets in a mouse model.

RESULTS—V5 treatment upregulated expression of anti-apoptotic proteins Bcl-2 and XIAP (X-linked inhibitor of apoptosis protein) by more than 3- and 11-fold and downregulated expression of apoptosis-inducing proteins Bax, Bad, and nuclear factor-κB–p65 by 10, 30, and nearly 50%, respectively. Treatment improved the recovered islet mass following collagenase digestion and isolation by 44% and in vitro glucose-responsive insulin secretion nearly fourfold. Following transplantation in streptozotocin-induced diabetic mice, 150 V5-treated islet equivalents functioned as well as 450 control untreated islet equivalents in normalizing blood glucose.

CONCLUSIONS—These studies indicate that inhibition of apoptosis by V5 significantly improves islet function following isolation and improves islet graft function following transplantation. Use of this reagent in clinical islet transplantation could have a dramatic impact on the number of patients that might benefit from this therapy and could affect long-term graft survival.
***Diabetes* 56:1259–1267, 2007**

Pancreatic islet transplantation holds great promise as a treatment for type 1 diabetes. Insulin independence has been accomplished using a glucocorticoid-free immunosuppression regimen but often requires transplantation of islets from two to four donors (1–3). Since there is a considerable shortage of pancreas donors suitable for islet isolation, relatively few diabetic patients have benefited from this form of therapy. More effective recovery of islets from donor pancreata would dramatically increase the number of patients that could be treated by islet transplantation and could improve long-term graft survival (4–6).

Following transplantation, islets undergo apoptosis and necrosis from transient local hypoxia, a lack of nutrient support (7,8), and hyperglycemia-induced toxicity (9,10). While use of fibroblast growth factor-2 (FGF-2) at the time of transplantation improves revascularization of islet grafts and facilitates their engraftment (11), this approach addresses only part of the problem. Collagenase digestion of the pancreas has been shown to induce apoptosis of isolated islets from anoikis and loss of cell-matrix interactions (12,13). In addition, islets express proinflammatory nuclear factor-κB (NF-κB)–dependent genes after isolation, amplifying apoptosis signaling and potentially inducing immunological rejection (14–16). Optimization of the isolation process to reduce islet stress has failed to improve recovery, leaving uncontrolled apoptosis as the main cause of poor islet yield (3,13,17).

Investigators have attempted to prevent β-cell apoptosis by transferring antiapoptosis molecules (A20, Bcl-2, the Iκβ [inhibitor of κβ] repressor, and X-linked inhibitor of apoptosis protein [XIAP]) and growth factors (hepatocyte and vascular endothelial) into islet grafts (18–27). In most cases, these genes have been delivered by recombinant adenovirus. This approach, however, is not without potential risk (28). Use of IGF-II (29), leptin (30), and 17 β-estradiol (31) has improved islet mass recovery and viability but has not affected the number of islets that are needed following transplantation to correct diabetes in

From the [1]Department of Surgery, Okayama University Graduate School of Medicine and Dentistry, Okayama, Japan; the [2]Department of Advanced Medicine in Biotechnology and Robotics, Nagoya University Graduate School of Medicine, Nagoya, Japan; the [3]Department of Transplant Surgery, Kyoto University Hospital, Kyoto, Japan; the [4]Department of Orthopaedic Surgery, Okayama University Graduate School of Medicine and Dentistry, Okayama, Japan; the [5]Institute for Frontier Medical Sciences, Kyoto University, Kyoto, Japan; [6]Rosalind Franklin Comprehensive Diabetes Center, Chicago Medical School, North Chicago, Illinois; the [7]Department of Biochemistry, Chosun University School of Medicine, Gwangju, Korea; the [8]Second Department of Surgery, Fujita Health University, Aichi, Japan; and the [9]Department of Surgery, University of Nebraska Medical Center, Omaha, Nebraska.

Address correspondence and reprint requests to Naoya Kobayashi, MD, PhD, Department of Surgery, Okayama University Graduate School of Medicine and Dentistry, 2-5-1 Shikata-cho, Okayama, 700-8558, Japan. E-mail: immortal@md.okayama-u.ac.jp.

Received for publication 2 December 2006 and accepted in revised form 29 January 2007.

Published ahead of print at http://diabetes.diabetesjournals.org on 7 February 2007. DOI: 10.2337/db06-1679.

Additional information for this article can be found in an online appendix at http://dx.doi.org/10.2337/db06-1679.

FGF-2, fibroblast growth factor-2; HBSS, Hank's balanced salt solution; IL, interleukin; KRBB, Krebs-Ringer balanced buffer; NF-κB, nuclear factor-κB; TNF-α, tumor necrosis factor-α; TUNEL, transferase-mediated dUTP nick-end labeling; XIAP, X-linked inhibitor of apoptosis protein.

mice. The caspase-3 inhibitor Z-DEVD-fmk (32) improves islet recovery and viability but inhibits only caspase-3. Whereas these methods have helped reduce apoptosis during islet isolation, few methods have been developed to reduce apoptosis after islet transplantation.

We examined the efficacy of the cell-permeable pentapeptide apoptosis inhibitor V5, which inhibits a wide range of caspases, on improving pancreatic islet recovery. This molecule binds Bax and prevents mitochondrial cytochrome c translocation (33), resulting in global inhibition of caspases through activation of NF-κB–dependent and BH1–4 genes (14,15,22). In this study, we demonstrate that culture of isolated islets with V5 improved islet recovery and their capacity for glucose-responsive insulin secretion. Use of FGF-2 and V5 decreased the number of islets needed to correct diabetes following transplantation threefold and allowed routine correction of glucose homeostasis in mice using islets from a single donor.

RESEARCH DESIGN AND METHODS

Peptide synthesis and preparation. Synthesis of a V5 was carried out at Sigma Genosis (Ishikari, Japan). The purity of the material was 98.8%, and the total amount of the product was 48.9 mg. Dried peptide powders were stored at −80°C and dissolved in fresh pure water for the experiments.

Islet isolation and culture. Male inbred Balb/C mice, 20 g and 10–12 weeks old, were used as pancreas donors. All the experiments performed were approved by the institutional ethical committee and were conducted according to its guidelines. Mouse islet isolation was performed with Hank's balanced salt solution (HBSS) (GibcoBRL, Grand island, NY), containing 2 mg/ml type-V collagenase (Sigma-Aldrich, St. Louis, MO), 2 mg/ml soybean trypsin inhibitor (Sigma-Aldrich), and 0.2% BSA (Sigma-Aldrich), using a modified Gotoh's method with Histopaque 1077-RPMI 1640 medium gradient (Sigma-Aldrich).

Islets were handpicked up under a microscope and cultured with RPMI-1640 (GibcoBRL) at 37°C and 5% CO_2 for in vitro analyses. Freshly isolated islets were used immediately for transplantation experiments. Islet viability was evaluated using a Live & Dead detection kit (Molecular Probes, Eugene, OR) in accordance with the manufacturer's instructions. Purity of islets was assessed by dithizone staining, and islet equivalents' yield was determined using a phase-contrast microscopy with a squared calibrated grid. One islet equivalent was equal to a spherical islet of 150 μm in diameter. ATP content of islets, directly after isolation and following 24 h of culture, was measured at SRL (Tokyo, Japan) using 500 islet-equivalent aliquots per experiment in three separate studies.

Measurement of mitochondrial activity of islets. Islets of 50 islet equivalents were cultured for 24 h with or without 100 μmol/l V5 in each well of six-well plates (BD Biosciences, San Jose, CA), and mitochondrial dehydrogenases activity of islets were comparatively measured using 0.5 mg/ml of MTT (3-[4,5-dimethylthiazol-2-yl]-2,5-diphenyl tetrazolium bromide) (MTT reagent; Sigma). Freshly isolated islets were used as a positive control (34). Three independent experiments were performed.

Detection of apoptosis of islets by annexin-V expression. Expression of annexin-V was measured in islets treated with or without 100 μmol/l V5 at 24 h of culture. Islets were washed twice with HBSS and dispersed to a single cell by gentle pipeting in trypsin-EDTA (Sigma-Aldrich). Single islet cells were washed twice with HBSS containing 10% newborn calf serum (Sigma-Aldrich) and labeled with an annexin V–enhanced green fluorescent protein apoptosis detection kit (MBL, Nagoya, Japan), according to the manufacturer's instructions, and analyzed by a MoFlo cell sorter (Dako-Cytomation, Tokyo, Japan). Apoptotic cells were identified by the fluorescence of enhanced green fluorescent protein. Freshly isolated islets were used as a control (3). Three independent experiments were performed.

Power blot analysis for apoptosis-associated molecules. Islets (1,000 islet equivalents) were cultured with RPMI-1640-S with or without V5 (100 μmol/l) for 24 h. Then, islets were washed with HBSS twice, rinsed with ice-cold lysis buffer of PBS containing 1.0% Triton X-100 (Sigma-Aldrich), sonicated for 30 s, and placed on ice for 10 min. Lysates were centrifuged at 15,000 rpm for 10 min at 4°C to exclude cellular debris. Protein concentrates were collected and analyzed for 50 apoptosis-associated molecules according to the manufacture's protocol (Clonotech, Tokyo, Japan). Three independent experiments were performed.

Measurement of insulin secretion, insulin content, and stimulation index of islets. Islets (10 islet equivalents/well of six-well plates) were cultured in RPMI-1640-S supplemented with or without V5 (100 μmol/l) in both standard and ultralow attachment plates (BD Bioscience, Tokyo, Japan). Islets were treated for 20 min in 2 ml of Krebs-Ringer balanced buffer (KRBB) (containing 143.0 mmol/l Na, 5.8 mmol/l K, 2.5 mmol/l Ca, 1.2 mmol/l Mg_2, 124.1 mmol/l Cl, 1.2 mmol/l PO-4, 1.2 mmol/l SO-4, 25 mmol/l HCO-3, 10 mmol/l HEPES, 0.2% BSA, and 3.3 or 25 mmol/l glucose) at pH 7.4 for RPMI-1640-S equilibration. Insulin secretion of the islets was measured under static incubation using a Mercodia mouse insulin enzyme-linked immunosorbent assay kit (Uppsala, Sweden) at 0, 24, 72, 120, and 168 h, as previously reported (35,36). Briefly, islets were first incubated at 37°C and 5% CO_2 for 2 h in KRBB with 3.3 mmol/l glucose, then in KRBB with 25 mmol/l glucose for 2 h, and finally in KRBB with 3.3 mmol/l glucose. Amount of insulin content of islets was measured at the end of static incubation. Three independent experiments were performed.

Transplantation experiments. Female inbred Balb/C mice, 20 g and 10 weeks old, received a single intraperitoneal injection of 220 mg streptozotocin per kg body wt. Mice with blood glucose levels >360 mg/dl on a minimum of two consecutive measurements were selected as recipients (34). Gelatinized microspheres for islet transplantation (30–50 μm in size) containing both FGF-2 (100 ng) and V5 (100 μmol/l) or FGF-2 (100 ng) only were prepared through glutaraldehyde cross-linking of an aqueous gelatin solution, as previously reported (37). For transplantation, freshly isolated islets were suspended in 10 μl RMPI-1640-S medium, embedded with the gelatinized microspheres, and then transplanted under the kidney capsule of diabetic mice.

Diabetic mice were divided into the following four groups: *1*) $n = 21$, transplantation with 150 islet equivalents obtained from one mouse prepared with FGF-2 only; *2*) $n = 21$, transplantation with 150 islet equivalents obtained from one mouse prepared with both FGF-2 and V5; *3*) $n = 21$, transplantation with 450 islet equivalents obtained from three mice prepared with FGF-2 only; and *4*) $n = 5$, animals received no islet transplants. Normal healthy mice were used as a positive control (group 5; $n = 5$).

In vivo evaluation after islet transplantation in diabetic mice. Blood glucose levels were monitored at regular intervals for 27 weeks. Normoglycemia was defined to be <126 mg/dl in at least two consecutive measurements. An intraperitoneal glucose tolerance test was performed at 24 weeks. Mice were fasted overnight and then glucose (1g/kg body wt) was injected intraperitoneally, as previously described (34). Nephrectomy was performed at 26 weeks in the mice of groups 1, 2, and 3, and total insulin content of the samples was measured per microgram graft (34).

Histological studies of kidneys bearing islet grafts. Kidneys bearing islet grafts were removed at 3 days and at 26 weeks after transplantation ($n = 3$ from groups 1, 2, and 3), fixed in 10% formalin for 24 h, and embedded in paraffin for hematoxylin-eosin staining, insulin staining, and transferase-mediated dUTP nick-end labeling (TUNEL) staining. Serial-matched paraffin sections were used for these stainings. Polyclonal anti-insulin guinea pig primary antibodies (Dakocytomation) were applied. Then, secondary antibody phycoethrin-labeled anti–guinea pig (Amersham Biosciences) was added. Green fluorescent nuclear counterstaining was used for all the samples. Immunofluorescent stained slides were observed under a confocal laser-scanning microscope (LSM510; Carl Zeiss) (34). An in situ cell death detection tetramethylrhodamine red kit (Roche, Mannheim, Germany) was used for TUNEL staining.

PCR analysis. For detection of inflammatory molecules, total RNA was extracted from kidneys bearing islet grafts 2 days after transplantation using RNA Trizol (Invitrogen), as previously reported (38). RT-PCR was performed at 22°C for 10 min and then at 42°C for 20 min using 1.0 μg RNA per reaction to ensure that the amount of cDNA amplified was proportional to the mRNA present in the original samples. The following specific primers were used: interleukin (IL)-1β (NM_008361), 5′-caggcaggcagtatcactca-3′ forward and 5′-agctcatatgggtccgacag-3 reverse; tumor necrosis factor (TNF)α (NM_01369), 5′-agtccgggcaggtctacttt-3 forward and 5′-ggtcactgtcccagcatctt-3 reverse; Bcl-2 (NM_009741), 5′-aggagcaggtgcctacaaga-3 forward and 5′-gcattttcccaccactgtct-3 reverse; and GAPDH (NM_008084) 5-acccagaagactgtggatgg-3 forward and 5′-cacattgggggtaggaacac-3 reverse.

Immunoelectron microscopic examination of kidneys bearing islet grafts. At 26 weeks, kidneys bearing islet grafts were harvested ($n = 3$ each from groups 1, 2, and 3) and fixed with 4% paraformaldehyde and 0.1% glutaraldehyde in 0.1 mol/l phosphate buffer at pH 7.4. Samples were embedded in LR White (London Resin, London, U.K.). Ultrathin sections on nickel grids were incubated with 6 mol/l urea in 0.1 mol/l glycine-HCl buffer (pH 3.5) for 5 min to etch the surface of sections. The grids were incubated with polyclonal anti-insulin–guinea pig primary antibodies (DakoCytomation) at 4°C overnight. After washing, the grids were incubated for 1.5 h with 10 nm colloidal gold-conjugated goat anti–guinea pig IgG (British Biocell Interna-

TABLE 1
Effect of V5 on mouse islets isolated in association with 12 h of cold ischemia and 30 min of warm ischemia

Experiments	V5	Islet yield	Islet viability (%)			ATP (pg/islet equivalent)	
			0 h	12 h	24 h	0 h	24 h
Cold ischemia	+	110.8 ± 9.4	93.3 ± 2.1	92.1 ± 2.3*	88.9 ± 3.8*	39.4 ± 8.2	129.3 ± 11.2*
	−	108.3 ± 10.8	92.4 ± 3.7	71.4 ± 6.4*	57.3 ± 5.6*	40.2 ± 7.9	68.4 ± 8.4*
Warm ischemia	+	83.5 ± 7.3	58.9 ± 10.6	46.0 ± 8.2§	39.2 ± 7.9*	19.8 ± 3.5	45.9 ± 8.5*
	−	82.3 ± 8.6	60.3 ± 9.2	37.8 ± 4.5†	14.8 ± 4.7*	21.6 ± 2.8	16.1 ± 5.8*

Data are means ± SE. *$P < 0.01$ for V5(+) vs. V5(−); †$P < 0.05$ for V5(+) vs. V5(−).

tional). The grids were washed, postfixed with 2% glutaraldehyde, rinsed with ddH2O, and dried. The sections were stained with 2% uranyl acetate for 15 min and 3% lead citrate for 1 min and observed with a Hitachi H-7100 transmission electron microscope (35).

Statistical analysis. Results were expressed as means ± SE. For comparisons between two groups, the paired or unpaired Student's *t* test (two tailed) was used. For multiple comparisons, the one-way ANOVA was used. Kaplan-Meier method was used to calculate the survival data. A *P* value <0.05 was considered significant when determined by the Mann-Whitney *U* test.

RESULTS

Effect of treatment with V5 on islet viability and function, as well as parameters associated with apoptosis in vitro. Pancreatic islet yield following isolation was 152.5 ± 3.46 islet equivalents per mouse. Islet viability immediately after isolation, and 12 and 24 h later in control culture, was 99.1 ± 0.7%, 81.0 ± 1.2%, and 72.0 ± 0.9%, respectively, whereas viability at the same time points after culture in the presence of 100 μmol/l V5 was 98.9 ± 0.6%, 95.4 ± 0.8%, and 93.5 ± 0.6%. To assess the effect of V5 on islets recovered under clinically relevant donor recovery conditions, we also evaluated the effect of V5 on mouse islets isolated in association with 12 h of cold ischemia and 30 min of warm ischemia. We found that V5 was effective in protecting mouse islets under these conditions (Table 1). Since apoptosis is often reflected in mitochondrial function, we assessed mitochondrial dehydrogenase activity 24 h after isolation. As shown in Fig. 1*A*, mitochondrial dehydrogenase activity was significantly greater in V5-treated islets (96.4 ± 1.5%) than that in control untreated islets (54.0 ± 5.7%). We also measured the expression of annexin-V, an early marker of apoptosis, 24 h after isolation. V5-treated islets expressed significantly less annexin-V (14.0%) than control untreated islets (58.5%) (Fig. 1*B–D*). A power blot was then performed to identify proteins significantly (more than twofold) altered in isolated islets after treatment for 24 h in V5. Power blot analysis screened over 50 proteins associated with apoptosis (Fig. 1*E*). Western blot analysis showed a 0.11-fold reduction in the expression of the pro-apoptotic protein Bax, a 0.34-fold reduction in Bad, and a 0.46-fold reduction in NF-κB–p65. Treatment of islets with V5 also generated an 11.76-fold upregulation in XIAP and a 3.31-fold increase in Bcl-2 expression (Fig. 1*E* and F).

To further investigate the effect of V5 on recovered islets, we analyzed glucose-responsive insulin secretion, or insulin secretion index, immediately after isolation and 24, 72, 120, and 168 h later. Since islets adherent to culture plates lose function quickly, analysis was performed on islets under both adherent and nonadherent conditions. V5-treated islets had a 2.7- to 3.7-fold higher insulin secretion index than control untreated islets at all time points under both adherent and nonadherent conditions (Fig. 2*A* and *B*), and V5-treated islets maintained their insulin content (128 ± 1 at 24 h and 76 ± 6 at 168 h under adherent culture conditions; 128 ± 3 at 24 h and 101 ± 5 at 168 h under nonadherent culture conditions) significantly better than untreated control islets (116 ± 5 at 24 h and 9 ± 2 at 168 h under adherent culture conditions; 117 ± 4 at 24 h and 80 ± 4 at 168 h under nonadherent culture conditions) (Fig. 2*C* and *D*), respectively.

Effect of V5 on recovered islets after transplantation. To investigate the effect of V5 treatment on recovered islets after transplantation, we transplanted V5-treated and control untreated islets into streptozotocin-induced diabetic mice. Transplantation procedures induce a meaningful grade of apoptosis, dramatically reducing the islet engraftment capacities and its survival by induction of the inflammatory reactions. We examined the potential prevention of apoptosis in vivo by microspheres containing V5 and FGF-2 within the islets grafts, 3 days after transplantation, by insulin staining and TUNEL assay. We found that the number of insulin-positive cells was significantly maintained by V5 treatment (150 control untreated islet equivalents: 51 ± 9 cells/high power field vs. 150 V5-treated islet equivalents: 202 ± 23 cells/high power field; Fig. 3*A–F* and *J*). Notably, a significantly larger number of TUNEL-positive cells were observed in control untreated islet grafts than found in V5-treated islets (Fig. 3*G–I* and *K*). V5 treatment significantly reduced inflammatory molecule IL-1β and TNF-α gene expression and enhanced Bcl-2 gene expression in islet grafts (Fig. 3).

In consistency with this, following transplantation of 150 V5-treated islet equivalents (recovered from one donor), normoglycemia was achieved in all diabetic recipients within 12 days and 100% 6-month survival obtained (Fig. 4*A* and *B*). In contrast, transplantation of 150 control untreated islet equivalents (recovered from one donor) failed to tightly control blood glucose levels, and 60% of diabetic recipients died 6 months after transplantation. Transplantation of 450 control untreated islet equivalents (recovered from three donors) corrected hyperglycemia to the same degree as transplantation of 150 V5-treated islet equivalents and produced a similar degree of blood glucose control to that after transplantation of 150 V5-treated islet equivalents following glucose challenge (Fig. 4*C*). Removal of kidneys bearing islet grafts 26 weeks after transplantation produced hyperglycemia in all transplanted mice, indicating that the islet grafts were responsible for correction of diabetes. Histological analysis of V5-treated islet grafts showed a comparatively equal amount of both total insulin content (16.1 ± 0.4 μg/graft), compared with those (16.7 ± 1.4 μg/graft) of V5-untreated 450 islet equivalents (Fig. 4*D*), and size of the functional islet grafts (Fig. 5*B*, *C*, *E*, and *F*). Insulin immunoelectron microscopy 26 weeks after transplantation showed β- cells with numerous secretory granules and well-preserved ultrastructure organelles following V5-treatment (Fig. 5*H* and *J*), whereas control untreated islet grafts showed

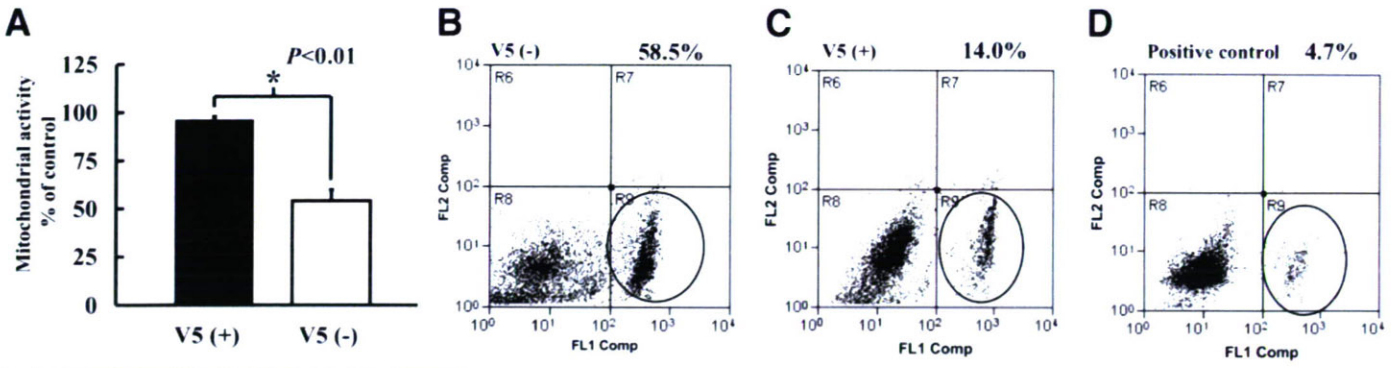

E

Lane1	Lane4	Lane7
Apaf-1	Btf	DAP Kinase
Ku70	GOK/Stim1	CAS
MST3	RIP2/RICK	DFF45
EB3	Selenocysteine Lyase	Peroxiredoxin V
Bcl-x	PI31	**Lane8**
		Mitosin
Bax	Bcl-2	Dlg
Lane2	**Lane5**	BMX
SLK	DNA Polymerase e catalytic	
SLK	IKAP	APP-BP1
Ku80	IKKb	DAP3
NF-kB p65	hILP/XIAP	TRADD
IKKg/NEMO	IkBa/MAD-3	**Lane9**
		Integrin a5
Bad	Bid	LRP
Lane3	**Lane6**	FIP-2
DNA Polymerase d	TopBP1	
RIP	DNA Ligase III	PKR
MST1	Nup88	Smac/DIABLO
Fas/CD95/APO 1	hILP/XIAP	
EB1	IkBe	
	FADD	

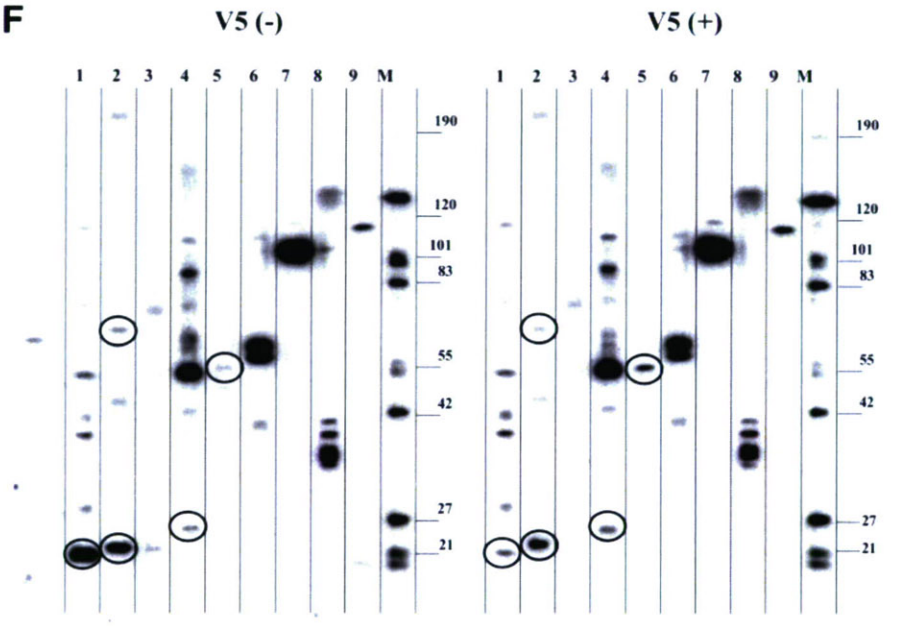

FIG. 1. Mitochondrial function, annexin-V expression, and power blot assay of the islets treated with V5. *A*: Comparative measurements of mitochondrial function of the islets at 24 h by an MTT assay. V5-treated islets showed significantly better function than untreated islets [$P < 0.01$ for V5 (+): 96.4 ± 1.5%] and V5 (−): 54.0 ± 5.7%). The value for islets immediately after isolation was 100%. *B–D*: Detection of annexin-V expression. V5-untreated islets revealed the high expression of annexin-V (58.5%) 24 h after isolation. The significantly lower expression of annexin-V (14.0%) was observed in the V5-treated islets at 24 h, which was relatively comparable with that of normal islets immediately after isolation (8.7%). *E*: List of the molecules assessed by a power blot study. *F*: The differential expression of the molecules in V5-treated or -untreated islets at 24 h. The marked reduction of the expression of pro-apoptotic proteins of Bax, Bad, and NF-κB p65 and the upregulated expression of XIAP and Bcl-2 were observed in V5-treated islets. The data are representative of three independent experiments.

fewer β-cells, each containing fewer insulin secretory granules and organelles (Fig. 5*G* and *J*).

DISCUSSION

Type 1 diabetes results from the loss of insulin-producing pancreatic β-cells by β-cell–specific autoimmune responses. Pancreatic islet transplantation is one possible method for the cure of diabetes; however, the shortage of human donor pancreata limits the widespread application of this procedure (1,5,6). Because a relatively large β-cell mass from two to four donor pancreata is needed to achieve normoglycemia in the recipient, it is crucial to develop treatments that would reduce loss of transplanted islets due to apoptosis and maximize use of the limited amount of donor tissue. Isolation of human islets is very stressful on the cells as it disrupts cell-cell and cell-matrix interactions and results in islet apoptosis (9,12,13,17, 32,38,39). Alterations in islet fine structure can be seen shortly after isolation and culture in vitro. Prevention of apoptosis has been a target to maintain islet mass for transplantation; for example, overexpression of XIAP (26) or A20 (23) in mouse islets by adenoviral vector–mediated delivery prevented early posttransplant apoptosis and reduced the islet cell mass needed to achieve normoglycemia. Although ex vivo gene transfer procedures using viral vectors are attractive, adenovirally transduced islets should be cultured to eliminate the risk of viral gene transfer to recipients. Thus, it would be beneficial to develop a simple, efficient method to protect islets from apoptosis and reduce the number of islets required for transplantation.

Bax is a member of the Bcl-2 family of proteins and plays a key role in the induction of apoptosis. In response to apoptotic stimuli, Bax translocates from the cytosol to mitochondria and causes release of apoptogenic factors (40). Inhibition of Bax would be extremely useful in islet culture immediately after isolation procedure. Ku70 plays an important role in DNA double-strand break repair in the nucleus (41). Ku70 binds Bax in the cytosol and inhibits its translocation into mitochondria (33). The Bax-binding

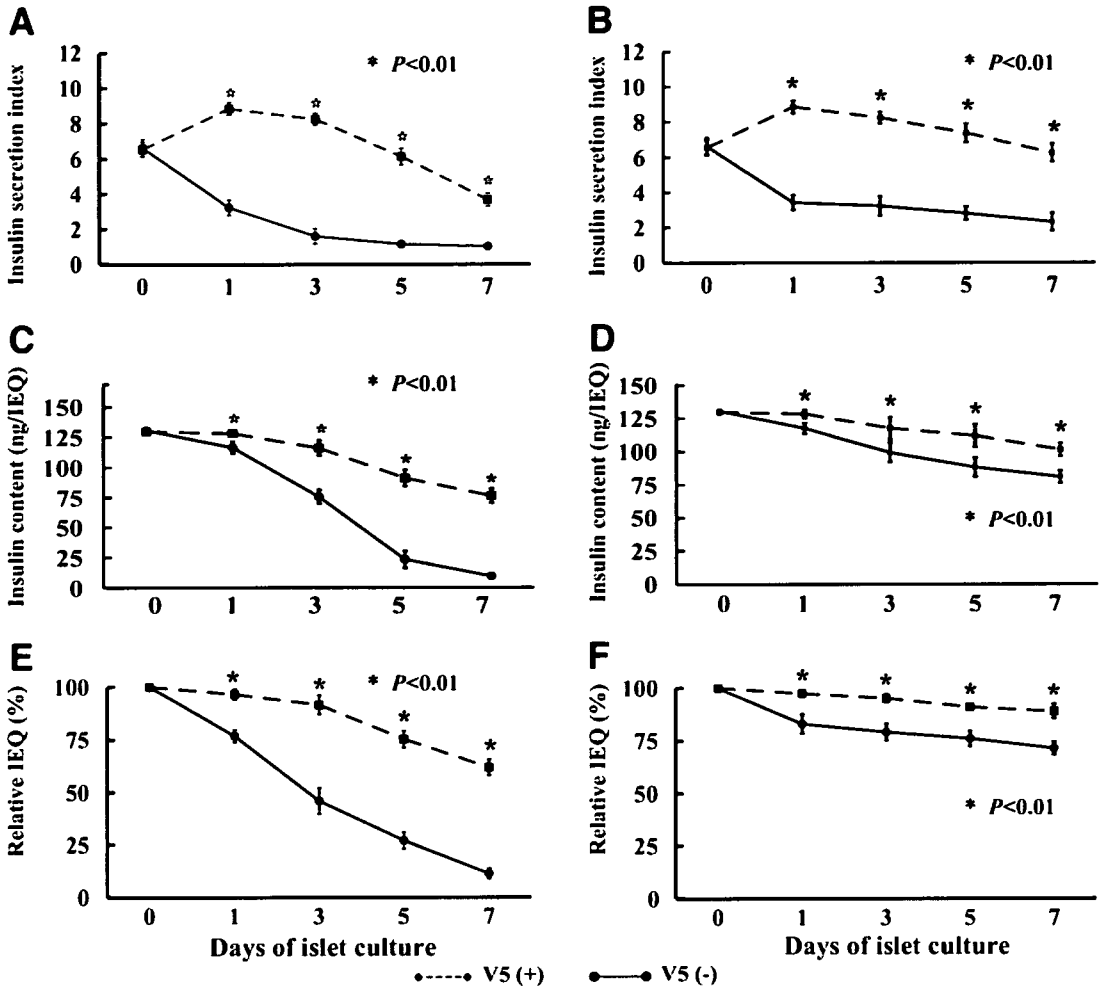

FIG. 2. Insulin secretion index and insulin content of islets. *A*: V5-treated islets showed significantly better insulin secretion index than V5-untreated islets at days 1, 3, 5, and 7. *C*: The insulin content was significantly higher in V5-treated islets at days 1, 3, 5, and 7 compared with V5-untreated islets. These data are representative of three independent experiments. *E*: Treatment of V5 allowed significantly favorable maintenance of islet mass at days 1, 3, 5, and 7. *B–F*: These findings, observed in adherent culture, were also confirmed in islets in floating culture using ultralow attachment dishes. IEQ, islet equivalent.

domain of human Ku70 consists of residues 578–583, and a pentapeptide (i.e.,V5) contained within these residues is cell permeable and suppressed Bax-mediated apoptotic cell death in several types of human cells, including hepatoma Hep3B cells and myeloid 32D (EpoR wt) cells (14). We previously found that V5 treatment of monkey hepatocyte cultures improved differentiated function and prolonged cell survival (42). In this study, we investigated the effect of V5 on islet viability and functionality during islet isolation and transplantation into diabetic mice.

First, we examined the effect of V5 on apoptosis of islets in vitro. We found that fluorescein isothyocyanate–labeled V5 (100 μmol/l) was uniformly taken up by islet cells within 3 h when added into the culture, and no cytotoxic effects were observed with a dose ≤500 μmol/l (data not shown). Treatment of islets isolated from Balb/c mice with V5 peptide significantly increased viability and inhibited apoptosis.

The mitochondrial metabolite, succinate, is a key metabolic mediator of glucose-stimulated preproinsulin gene transcription and translation (43). Therefore, we examined mitochondrial function in V5-treated islets and found that mitochondrial function was increased by ~42% compared with untreated islets. Preservation of mitochondrial function in β-cells is critical for preserving their capacity to produce, store, and secrete insulin. V5 treatment significantly enhanced ATP levels in both 12-h cold preserved and 30-min warm preserved islets (Table 1) and markedly reduced apoptosis. Consistent with these findings, glucose-responsive insulin secretion was also increased by 2.7- to 3.7-fold in V5-treated islets. Islets treated with V5 maintained the insulin content of freshly isolated islets, even after 1 week of culture. Since islet culture seems to be an important step in the islet transplantation, the use of V5 might constitute an important tool for maintaining more viable islets with enhanced insulin secretion over the conventional cultures, floating better than adherent culture with matrices. Second, we examined the expression of proteins involved in the regulation of apoptosis in V5-treated islets. We found that the expression of pro-apoptotic molecules Bax, Bad, and NF-κB was markedly reduced, and the expression of anti-apoptotic molecules XIAP and Bcl-2 was upregulated. XIAP has previously been shown to improve β-cell growth, survival, and metabolic function during stress (35,44,45) and affects Akt/protein kinase B phosphorylation (36,45), modulating Bad, caspase-9, Bcl-2, cyclic AMP–response element-binding

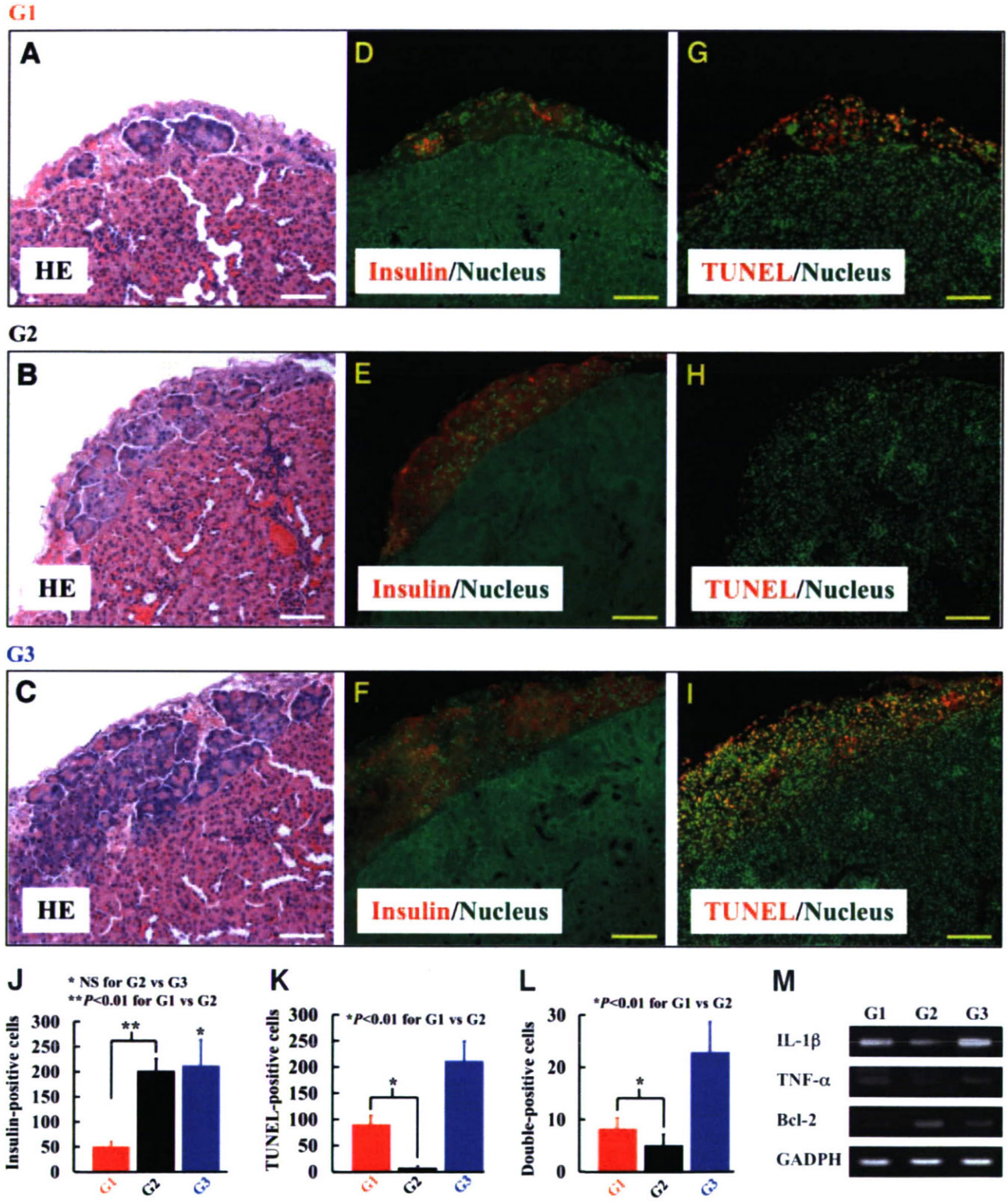

FIG. 3. Histological study of islets transplanted into the subrenal capsule in diabetic mice at 3 days. *A–C* (hematoxylin and eosin staining): A few clusters of islets were found in the graft of V5-untreated 150 islet equivalents (group 1: obtained from one donor), but much larger clusters were detected in that of V5-treated 150 islet equivalents (group 2: obtained from one donor). Amounts of islets were found in the graft of V5-untreated 450 islet equivalents (group 3: obtained from three donors), which served as a positive control. *D–F* (insulin staining): A few insulin-expressing cells, indicated by a red signal, were observed in the group 1 graft; in contrast, the group 2 graft showed significantly more insulin-positive cells, in which insulin intensity was stronger than in the cells in the group 3 graft. The observation was confirmed by counting the cell numbers of 10 different sections of each sample ($n = 3$) (*J*). The number of insulin-positive cells was 51.3 ± 8.7 for group 1, 202.1 ± 23.4 for group 2, and 212.5 ± 51.1 for group 3. *G–I* (TUNEL staining): Significantly higher ratios of TUNEL-positive cells, indicated by a red signal, were observed in the grafts of groups 1 and 3 compared with the group 2 graft. *K*: The number of TUNEL-positive cells was counted in 10 different sections of each sample ($n = 3$), and it was 91.2 ± 15.7 cells for group 1, 8.1 ± 3.1 for group 2, and 211.7 ± 37.6 for group 3. Scale bars = 200 μm. *L*: The number of double- (TUNEL- and insulin-) positive cells was counted in 10 different sections of each sample ($n = 3$), and it was 8.3 ± 2.0 cells for group 1, 5.1 ± 2.0 for group 2, and 22.9 ± 5.8 for group 3. Scale bars = 200 μm. *M*: V5 treatment significantly depressed inflammatory molecule IL-1β and TNF-α gene expression and enhanced Bcl-2 expression in islet grafts 2 days after transplantation.

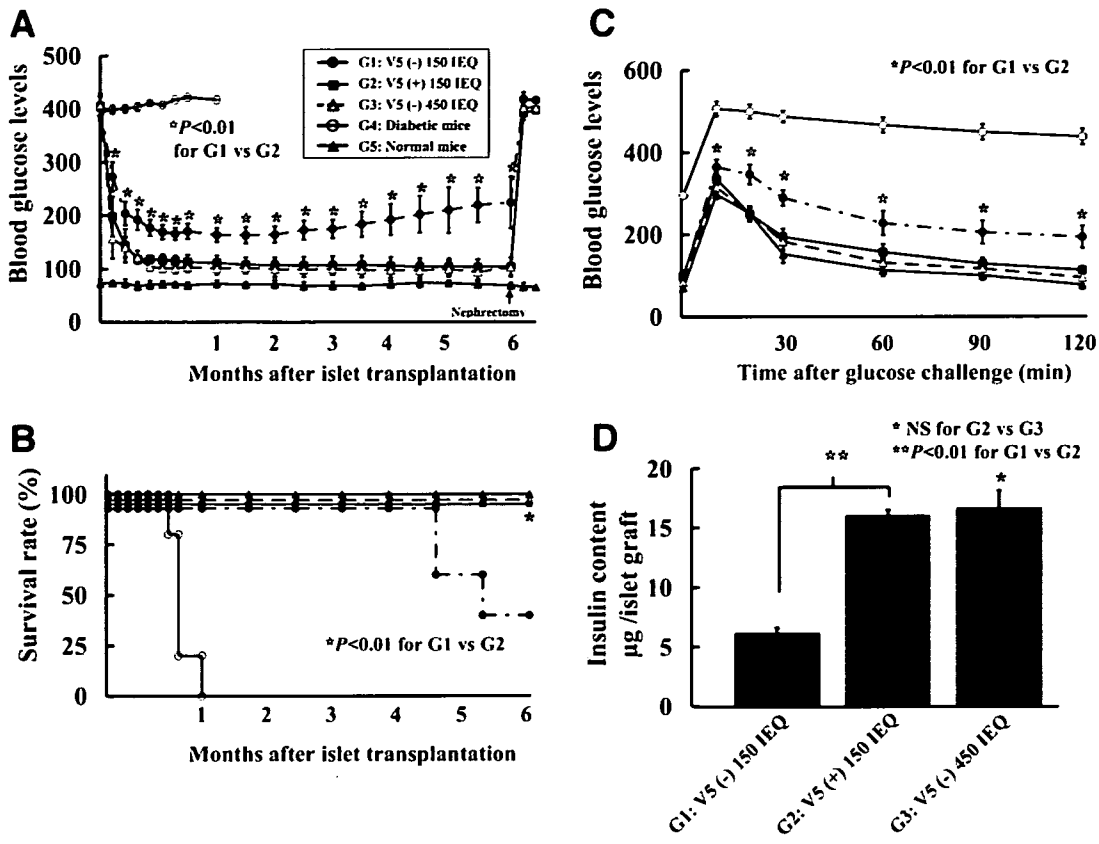

FIG. 4. Blood glucose levels, survival rate, and glucose challenge tests after islet transplantation and insulin content of islet grafts. *A*: Transplantation of V5-treated 150 islet equivalents (group 2) perfectly controlled the blood glucose levels of diabetic mice for 6 months; levels were comparable with those observed in group 3. *B*: All mice in group 2 survived for 6 months. *C*: Intraperitoneal glucose tolerance test performed at 24 weeks. The mice with group 2 showed a normal profile of blood glucose levels after glucose challenge. *D*: Insulin content of islet grafts. Significantly higher insulin content was observed in the group 2 graft (16.1 ± 0.4 mg/graft), which was comparable with that of the group 3 graft (16.7 ± 1.4), in comparison with the group 1 graft (6.2 ± 0.2). IEQ, islet equivalent.

protein, and insulin receptor substrate-1 downstream. These changes may help to protect V5-treated islets from apoptosis and increase graft survival. The beneficial effects of XIAP have been reported. Overexpression of XIAP markedly enhanced β-cell survival and functional recovery of islets in hypoxia- and cytokine-induced injury in vitro (27). Overexpression of XIAP in human islets reversed the negative effects of immunosuppressive drugs on insulin secretion and cell viability (46). Recently, it was reported that XIAP overexpression in human islets prevented posttransplant apoptosis and reduced the islet mass required to treat diabetes (26).

These promising in vitro results suggested that V5 treatment might preserve the islet mass in grafts and thus reduce the number of islets needed to obtain insulin independence. Local hypoxia and lack of nutrients can cause apoptosis in islet transplants (8). Early vascularization of islet grafts can overcome these problems and facilitate islet engraftment. We have previously found that use of gelatinized microspheres containing slow-release, cross-linked FGF-2 that persists for ~2 weeks produced rapid islet revascularization at the site of implantation (37). In those mouse islet transplantation studies, islet graft function was improved by improved vascularization. However, we also encountered considerable transplantation-associated apoptosis that resulted in loss of islet mass (11). Therefore, in this study, we transplanted islets embedded in microspheres containing FGF-2, to enhance vascularization, and V5, to reduce apoptosis, and found that apoptosis was decreased and the number of insulin-positive cells was increased in grafts containing islets treated with V5. When we embedded 150 islet equivalents within FGF-2–conjugated microspheres along with V5, diabetes was remitted within 12 days in streptozotocin-induced diabetic mice, similar to the results seen in mice transplanted with 450 islet equivalents with FGF-2 only, suggesting that normoglycemia could be achieved with islets from a single donor if V5 is provided. Interestingly, V5 treatment significantly depressed inflammatory molecule IL-1β and TNF-α gene expression in islet grafts. We found that V5 treatment similarly affected allogenic islets following transplantation in preliminary studies (supplementary Fig. 1 [available in an online appendix at http://dx.doi.org/10.2337/db06-1679]). We next plan to explore methods to protect transplanted islets from autoimmune attack and early recurrence of diabetes following allogeneic islet transplantation.

In conclusion, we have shown that treatment of islets with V5 increases islet viability, enhances islet function, and prevents apoptosis. Transplantation of islets along with FGF-2 and V5 allowed a smaller islet mass (single-donor pancreas) to be used for transplantation; normoglycemia was achieved and insulin content and islet function were preserved posttransplantation. Timed release of V5, perhaps by gelatinization, may result in long-term prevention of apoptosis and improve outcomes in human islet transplantation.

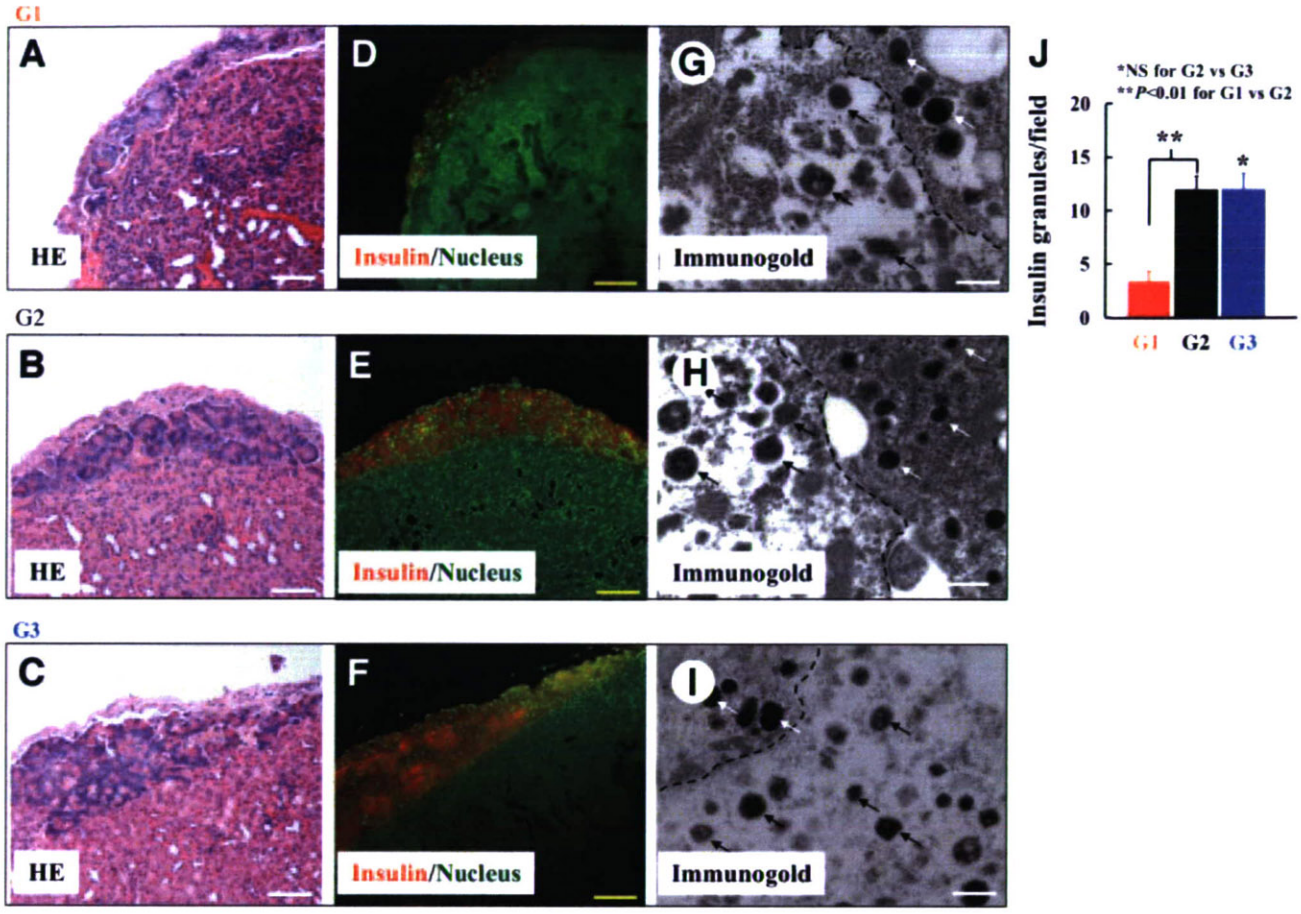

FIG. 5. Histological study of islets transplanted into the subrenal capsule in diabetic mice at 6 months. *A–C* (HE staining): Quite a few clusters of islets were found in the group 1 graft, but islet clusters were properly maintained in the group 2 graft, which was comparable with those in group 3 islets. Scale bars = 200 μm. *D–F* (insulin staining): Significantly more insulin-positive cells were observed in the group 2 graft than in the group 1 graft, which were comparable with the group 3 graft. Scale bars = 200 μm. *G–J* (transmission electron microscopy–immunogold staining): Numerous insulin secretory granules and well-preserved ultrastructural organelles were observed in the group 2 graft (12.0 ± 1.2 granules/field) when the grafts of group 1 (3.4 ± 0.09) and group 3 (12.0 ± 1.5) were considered. Such insulin granules were present in the apical zone of the β-cells in the group 2 graft. Black arrows indicate the insulin secretory granules labeled by immunogold, and white arrows show the glucagons granules (*J*). Scale bars = 300 nm. These data are representative of three different samples.

ACKNOWLEDGMENTS

The work presented in this paper was supported in part by the Ministry of Education, Science, and Culture and the Ministry of Economy and Industry, Japan; by Life Science Project of 21st Century, Japan; by a Grant-in-Aid for Scientific Research (B) of the Japan Society for the Promotion of Science (to N.K.); by the American Diabetes Association; by National Institutes of Health Grant 1R21DK60192; and by Canadian Institutes of Health Research Grant 89687 (to H.S.J.).

We thank Dr. Ann Kyle for editorial assistance and Tae Yamanishi for her valuable technical assistance, providing with the histological assessment.

REFERENCES

1. Shapiro AM, Lakey JR, Ryan EA, Korbutt GS, Toth E, Warnock GL, Kneteman NM, Rajotte RV: Islet transplantation in seven patients with type 1 diabetes mellitus using a glucocorticoid-free immunosuppressive regimen. *N Engl J Med* 343:230–238, 2000
2. Ryan EA, Lakey JR, Rajotte RV, Korbutt GS, Kin T, Imes S, Rabinovitch A, Elliott JF, Bigam D, Kneteman NM, Warnock GL, Larsen I, Shapiro AM: Clinical outcomes and insulin secretion after islet transplantation with the Edmonton protocol. *Diabetes* 50:710–719, 2001
3. Cattan P, Berney T, Schena S, Molano RD, Pileggi A, Vizzardelli C, Ricordi C, Inverardi L: Early assessment of apoptosis in isolated islets of Langerhans. *Transplantation* 71:857–862, 2001
4. Shapiro AM, Ricordi C: Unraveling the secrets of single donor success in islet transplantation. *Am J Transplant* 4:295–298, 2004
5. Matsumoto S, Okitsu T, Iwanaga Y, Noguchi H, Nagata H, Yonekawa Y, Yamada Y, Fukuda K, Tsukiyama K, Suzuki H, Kawasaki Y, Shimodaira M, Matsuoka K, Shibata T, Kasai Y, Maekawa T, Shapiro J, Tanaka K: Insulin independence after living-donor distal pancreatectomy and islet allotransplantation. *Lancet* 365:1642–1644, 2005
6. Hering BJ, Kandaswamy R, Ansite JD, Eckman PM, Nakano M, Sawada T, Matsumoto I, Ihm SH, Zhang HJ, Parkey J, Hunter DW, Sutherland DE: Single-donor, marginal-dose islet transplantation in patients with type 1 diabetes. *JAMA* 293:830–835, 2005
7. Paraskevas S, Aikin R, Maysinger D, Lakey JR, Cavanagh TJ, Hering B, Wang R, Rosenberg L: Activation and expression of ERK, JNK, and p38 MAP-kinases in isolated islets of Langerhans: implications for cultured islet survival. *FEBS Lett* 455:203–208, 1999
8. Ilieva A, Yuan S, Wang RN, Agapitos D, Hill DJ, Rosenberg L: Pancreatic islet cell survival following islet isolation: the role of cellular interactions in the pancreas. *J Endocrinol* 161:357–364, 1999
9. Davalli AM, Scaglia L, Zangen DH, Hollister J, Bonner-Weir S, Weir GC: Vulnerability of islets in the immediate posttransplantation period: dynamic changes in structure and function. *Diabetes* 45:1161–1167, 1996
10. Biarnes M, Montolio M, Nacher V, Raurell M, Soler J, Montanya E: β-cell death and mass in syngeneically transplanted islets exposed to short- and long-term hyperglycemia. *Diabetes* 51:66–72, 2002
11. Rivas-Carrillo JD, Navarro-Alvarez N, Soto-Gutierrez A, Okitsu T, Chen Y, Tabata Y, Misawa H, Noguchi H, Matsumoto S, Tanaka N, Kobayashi N: Amelioration of diabetes in mice after single-donor islet transplantation using the controlled release of gelatinized FGF-2. *Cell Transplant* 15:939–944, 2006

12. Thomas FT, Contreras JL, Bilbao G, Ricordi C, Curiel D, Thomas JM: Anoikis, extracellular matrix, and apoptosis factors in isolated cell transplantation. *Surgery* 126:299–304, 1999
13. Thomas F, Wu J, Contreras JL, Smyth C, Bilbao G, He J, Thomas J: A tripartite anoikis-like mechanism causes early isolated islet apoptosis. *Surgery* 130:333–338, 2001
14. Hengartner MO: The biochemistry of apoptosis. *Nature* 407:770–776, 2000
15. Hayden MS, Ghosh S: Signaling to NF-kappaB. *Genes Dev* 18:2195–2224, 2004
16. Hammonds P, Beggs M, Beresford G, Espinal J, Clarke J, Mertz RJ: Insulin-secreting beta-cells possess specific receptors for interleukin-1 beta. *FEBS Lett* 261:97–100, 1990
17. Paraskevas S, Maysinger D, Wang R, Duguid TP, Rosenberg L: Cell loss in isolated human islets occurs by apoptosis. *Pancreas* 20:270–276, 2000
18. Zhang N, Richter A, Suriawinata J, Harbaran S, Altomonte J, Cong L, Zhang H, Song K, Meseck M, Bromberg J, Dong H: Elevated vascular endothelial growth factor production in islets improves islet graft vascularization. *Diabetes* 53:963–970, 2004
19. Rabinovitch A, Suarez-Pinzon W, Strynadka K, Ju Q, Edelstein D, Brownlee M, Korbutt GS, Rajotte RV: Transfection of human pancreatic islets with an anti-apoptotic gene (*bcl-2*) protects β-cells from cytokine-induced destruction. *Diabetes* 48:1223–1229, 1999
20. Plesner A, Liston P, Tan R, Korneluk RG, Verchere CB: The X-linked inhibitor of apoptosis protein enhances survival of murine islet allografts. *Diabetes* 54:2533–2540, 2005
21. Lopez-Talavera JC, Garcia-Ocana A, Sipula I, Takane KK, Cozar-Castellano I, Stewart AF: Hepatocyte growth factor gene therapy for pancreatic islets in diabetes: reducing the minimal islet transplant mass required in a glucocorticoid-free rat model of allogeneic portal vein islet transplantation. *Endocrinology* 145:467–474, 2004
22. Hui H, Dotta F, Di Mario U, Perfetti R: Role of caspases in the regulation of apoptotic pancreatic islet beta-cells death. *J Cell Physiol* 200:177–200, 2004
23. Grey ST, Longo C, Shukri T, Patel VI, Csizmadia E, Daniel S, Arvelo MB, Tchipashvili V, Ferran C: Genetic engineering of a suboptimal islet graft with A20 preserves beta cell mass and function. *J Immunol* 170:6250–6256, 2003
24. Giannoukakis N, Rudert WA, Trucco M, Robbins PD: Protection of human islets from the effects of interleukin-1beta by adenoviral gene transfer of an Ikappa B repressor. *J Biol Chem* 275:36509–36513, 2000
25. Garcia-Ocana A, Takane KK, Reddy VT, Lopez-Talavera JC, Vasavada RC, Stewart AF: Adenovirus-mediated hepatocyte growth factor expression in mouse islets improves pancreatic islet transplant performance and reduces beta cell death. *J Biol Chem* 278:343–351, 2003
26. Emamaullee JA, Rajotte RV, Liston P, Korneluk RG, Lakey JR, Shapiro AM, Elliott JF: XIAP overexpression in human islets prevents early posttransplant apoptosis and reduces the islet mass needed to treat diabetes. *Diabetes* 54:2541–2548, 2005
27. Emamaullee J, Liston P, Korneluk RG, Shapiro AM, Elliott JF: XIAP overexpression in islet beta-cells enhances engraftment and minimizes hypoxia-reperfusion injury. *Am J Transplant* 5:1297–1305, 2005
28. Marshall E: Gene therapy death prompts review of adenovirus vector. *Science* 286:2244–2245, 1999
29. Robitaille R, Dusseault J, Henley N, Rosenberg L, Halle JP: Insulin-like growth factor II allows prolonged blood glucose normalization with a reduced islet cell mass transplantation. *Endocrinology* 144:3037–3045, 2003
30. Okuya S, Tanabe K, Tanizawa Y, Oka Y: Leptin increases the viability of isolated rat pancreatic islets by suppressing apoptosis. *Endocrinology* 142:4827–4830, 2001
31. Contreras JL, Smyth CA, Bilbao G, Young CJ, Thompson JA, Eckhoff DE: 17beta-Estradiol protects isolated human pancreatic islets against proinflammatory cytokine-induced cell death: molecular mechanisms and islet functionality. *Transplantation* 74:1252–1259, 2002
32. Nakano M, Matsumoto I, Sawada T, Ansite J, Oberbroeckling J, Zhang HJ, Kirchhof N, Shearer J, Sutherland DE, Hering BJ: Caspase-3 inhibitor prevents apoptosis of human islets immediately after isolation and improves islet graft function. *Pancreas* 29:104–109, 2004
33. Sawada M, Hayes P, Matsuyama S: Cytoprotective membrane-permeable peptides designed from the Bax-binding domain of Ku70. *Nat Cell Biol* 5:352–357, 2003
34. Narushima M, Kobayashi N, Okitsu T, Tanaka Y, Li SA, Chen Y, Miki A, Tanaka K, Nakaji S, Takei K, Gutierrez AS, Rivas-Carrillo JD, Navarro-Alvarez N, Jun HS, Westerman KA, Noguchi H, Lakey JR, Leboulch P, Tanaka N, Yoon JW: A human beta-cell line for transplantation therapy to control type 1 diabetes. *Nat Biotechnol* 23:1274–1282, 2005
35. Blume-Jensen P, Hunter T: Oncogenic kinase signalling. *Nature* 411:355–365, 2001
36. Asselin E, Mills GB, Tsang BK: XIAP regulates Akt activity and caspase-3-dependent cleavage during cisplatin-induced apoptosis in human ovarian epithelial cancer cells. *Cancer Res* 61:1862–1868, 2001
37. Tabata Y, Hijikata S, Muniruzzaman M, Ikada Y: Neovascularization effect of biodegradable gelatin microspheres incorporating basic fibroblast growth factor. *J Biomater Sci Polym Ed* 10:79–94, 1999
38. Berney T, Molano RD, Cattan P, Pileggi A, Vizzardelli C, Oliver R, Ricordi C, Inverardi L: Endotoxin-mediated delayed islet graft function is associated with increased intra-islet cytokine production and islet cell apoptosis. *Transplantation* 71:125–132, 2001
39. Aikin R, Rosenberg L, Paraskevas S, Maysinger D: Inhibition of caspase-mediated PARP-1 cleavage results in increased necrosis in isolated islets of Langerhans. *J Mol Med* 82:389–397, 2004
40. Wolter KG, Hsu YT, Smith CL, Nechushtan A, Xi XG, Youle RJ: Movement of Bax from the cytosol to mitochondria during apoptosis. *J Cell Biol* 139:1281–1292, 1997
41. Walker JR, Corpina RA, Goldberg J: Structure of the Ku heterodimer bound to DNA and its implications for double-strand break repair. *Nature* 412:607–614, 2001
42. Tanaka K, Kobayashi N, Gutierrez AS, Rivas-Carrillo JD, Navarro-Alvarez N, Chen Y, Narushima M, Miki A, Okitsu T, Noguchi H, Tanaka N: Prolonged survival of mice with acute liver failure with transplantation of monkey hepatocytes cultured with an antiapoptotic pentapeptide V5. *Transplantation* 81:427–437, 2006
43. Leibowitz G, Khaldi MZ, Shauer A, Parnes M, Oprescu AI, Cerasi E, Jonas JC, Kaiser N: Mitochondrial regulation of insulin production in rat pancreatic islets. *Diabetologia* 48:1549–1559, 2005
44. Song G, Ouyang G, Bao S: The activation of Akt/PKB signaling pathway and cell survival. *J Cell Mol Med* 9:59–71, 2005
45. Datta SR, Brunet A, Greenberg ME: Cellular survival: a play in three Akts. *Genes Dev* 13:2905–2927, 1999
46. Hui H, Khoury N, Zhao X, Balkir L, D'Amico E, Bullotta A, Nguyen ED, Gambotto A, Perfetti R: Adenovirus-mediated XIAP gene transfer reverses the negative effects of immunosuppressive drugs on insulin secretion and cell viability of isolated human islets. *Diabetes* 54:424–433, 2005

Luminescence 2007; 22: 455–461
Published online 4 July 2007 in Wiley InterScience (www.interscience.wiley.com) DOI: 10.1002/bio.984 *ORIGINAL RESEARCH*

Development of a novel neodymium compound for *in vivo* fluorescence imaging

Kazuki Aita, Takashi Temma, Yuji Kuge and Hideo Saji*

Department of Patho-functional Bioanalysis, Graduate School of Pharmaceutical Sciences, Kyoto University, Japan

Received 17 November 2006; revised 12 April 2007; accepted 12 April 2007

ABSTRACT: We developed a novel fluorescent probe that contains the neodymium(III) complex moiety and fluorescein moiety. This probe can emit long-lived near-infrared luminescence derived from a Nd ion through excitation of the fluorescein moiety with visible light (λ_{ex} = 488 nm, λ_{em} = 880 nm, lifetime = 2.3 μs). These results indicate the possibility of the probe as a candidate for *in vivo* fluorescence molecular imaging. Copyright © 2007 John Wiley & Sons, Ltd.

KEYWORDS: neodymium; near-infrared; fluorescein; energy transfer; long-lived luminescence

INTRODUCTION

Molecular imaging is a rapidly emerging biomedical research field that may be defined as the visual representation, characterization and quantification of biological processes at the cellular and subcellular levels within a living organism (1–3). As a technique of molecular imaging, fluorescence imaging attracts great interest.

In vivo fluorescence imaging, however, has several points that need to be considered, such as the permeability of the emission light, the background from scattered and reflected excitation light and self-fluorescence from tissues. To overcome such problems, the development of novel *in vivo* fluorescent probes has been required.

Near-infrared (NIR) light (700–1000 nm) has a potential for *in vivo* imaging. Provided that NIR light is used as emission light, it can permeate the body without intense absorbance and scatter by tissues (4) to offer a solution to problems such as permeability and background. In addition it has another advantage, that most biological compounds in living systems have no self-fluorescence in the NIR region.

Scattered and reflected light derived from excitation light are other obstacles, increasing background noise. Fortunately, background noise from excitation light can be removed by appropriate filters, provided that the difference between the excitation and emission wavelengths of the probe (Stoke's shift) is large enough; therefore, fluorescent probes with a large Stoke's shift have the potential to increase the S/N ratio in *in vivo* fluorescent imaging. However, most previously reported NIR probes (5–7) had an organic fluorescence centre with a small Stoke's shift ineffective for removing noise.

Consequently, we planned to develop a new fluorescent probe by chelating a neodymium (Nd) ion in its fluorescent centre for *in vivo* fluorescence imaging. Nd complexes have luminescence originating from $^4F_{3/2}$ to $^4I_{9/2}$ transition in the NIR region of 880 nm (8–10), unlike other lanthanide ions (e.g. Eu and Tb), and their Stoke's shift exceeds 200 nm, which is nearly 10 times larger than typical fluorescent dyes (fluorescein and rhodamine have Stoke's shifts of ~25 nm and ~20 nm, respectively). Such a favourable characteristic can increase the S/N ratio with the use of appropriate filters. In addition, the lifetime of lanthanide luminescence reaches the microsecond (μs) or millisecond (ms) order in contrast to the nanosecond (ns) order of organic fluorophores, making it possible to further cut down noise by time-resolved fluorescence imaging (4, 11).

As a chelating moiety, 1,4,7,10-tetraazacyclododecane-1,4,7,10-tetraacetic acid (DOTA) was selected, because DOTA and a Nd^{3+} ion form a highly stable complex [the log K value of Nd^{3+} and $DOTA^{4-}$ is 25.69 (12)] due to the tight coordination of DOTA with eight positions at maximum. This implies that the complex is not susceptible to metabolic degradation in living systems (13).

To excite a Nd ion, an antenna moiety, a sensitizing chromophore, is required in the structure because of the low absorbance of lanthanide f–f transitions (14). Thus, we selected fluorescein as the antenna moiety because of its long, less harmful excitation wavelength (~500 nm) and previous success in transferring energy to Nd (14). Moreover, it is also important that fluorescein is widely used in various fields, is highly soluble in water and can be easily modified for use in follow-up studies (15, 16).

*Correspondence to: H. Saji, Department of Patho-Functional Bioanalysis, Graduate School of Pharmaceutical Sciences, Kyoto University, Japan.
E-mail: hsaji@pharm.kyoto-u.ac.jp

Contract/grant sponsor: 21st Century COE Programme, Japan.

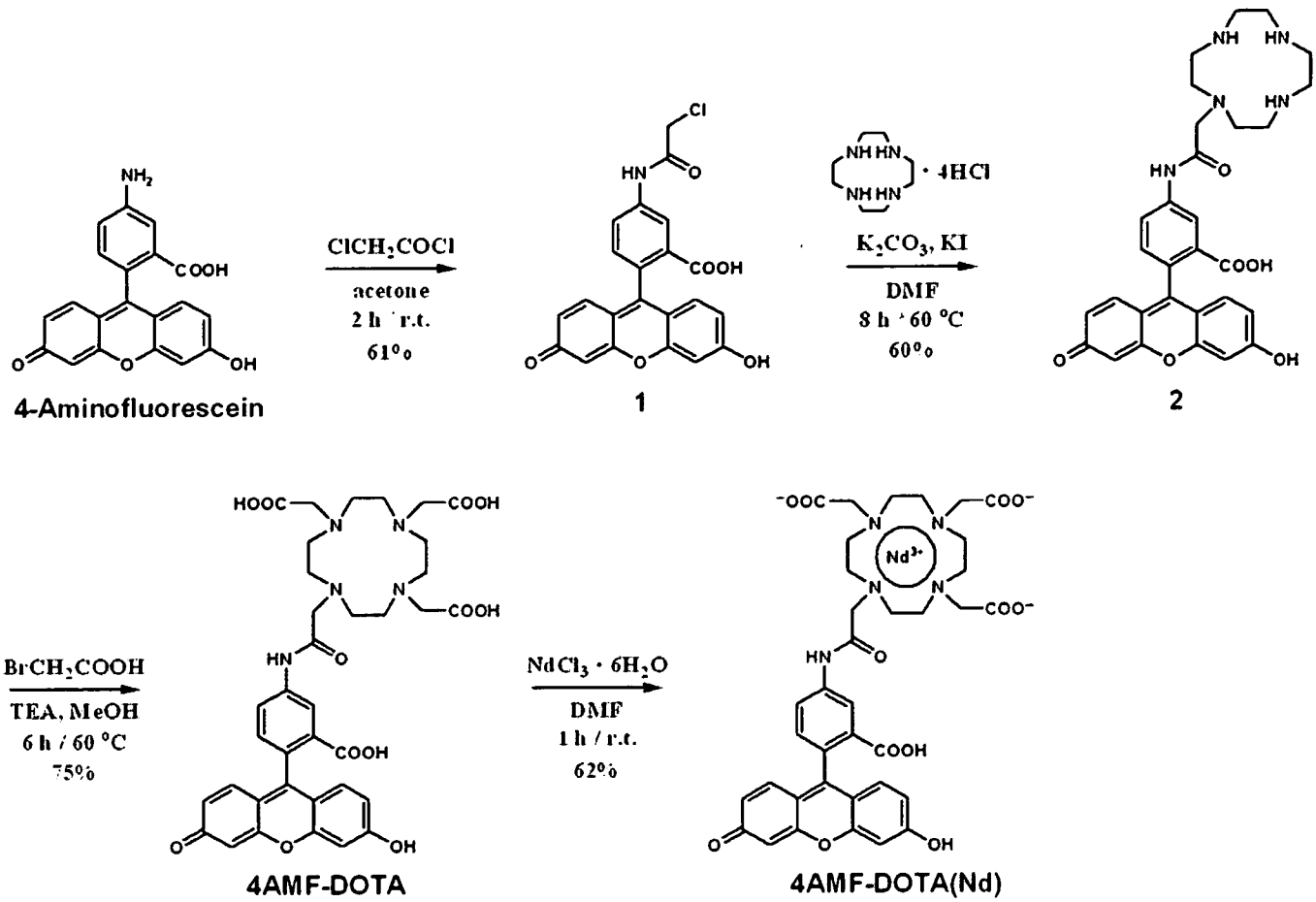

Scheme 1. Synthetic reaction scheme for 4AMF-DOTA(Nd).

In this study, we synthesized 4AMF-DOTA(Nd) including the Nd-DOTA (1,4,7,10-tetraazacyclododecane-1,4,7,10-triacetic acid) complex and fluorescein as a NIR fluorescent probe (Scheme 1), and investigated its chemical and physical features.

MATERIALS AND METHODS

Materials

All chemicals used in this study were commercial products of the highest purity and were further purified by standard methods if necessary.

Instruments

FT-IR spectra were recorded using a Jasco FT/IR-4100 (Nihon Bunko Inc., Tokyo, Japan). UV-vis spectra were measured using a Hitachi U2001 (Hitachi High-Tech Manufacturing & Service Corp., Ibaraki, Japan). Electrospray mass spectral (ESI–MS) measurements were performed on a SHIMADZU LC-MS2010 EV (Shimadzu Corp., Kyoto, Japan). ^{1}H-NMR spectra were recorded on a JEOL JNM-AL400 (JEOL Ltd, Tokyo, Japan). Fluorescence spectroscopy was performed with a Fluorolog-3 (Horiba Jobin Yvon Inc., Kyoto, Japan). The slit width was 10 nm for both excitation and emission. Time-resolved fluorescence spectra were recorded on a Fluorolog-3 with Phosphorescence (Horiba Jobin Yvon). The slit width was 12 nm for both excitation and emission. In both fluorescence spectra measurements, the photomultiplier voltage was 1450 V.

Fluorescence emission and excitation spectral measurements

The fluorescence emission spectra of 4AMF-DOTA(Nd) (10 μmol/L) without delay time were measured in 10 mmol/L Tris–HCl buffer, pH 8.0, 10 mmol/L Britton–Robinson buffer, pH 2–11, MeOH, EtOH and DMSO (each organic solvent contained 0.1% v/v Et_3N) at 25°C, following excitation at 488, 498, 504 and 523 nm in the buffers, MeOH, EtOH and DMSO, respectively. Excitation spectra were obtained at an emission wavelength of 870 nm.

Time-delayed luminescence spectral measurement

The time-delayed luminescence spectra of 4AMF-DOTA(Nd) (10 μmol/L) were measured in 10 mmol/L Tris–HCl buffer, pH 8.0, at 25°C, following excitation at 488 nm. A delay time of 7 μs and a gate time of 100 μs were used.

UV-visible absorption spectral measurement

The absorption spectral changes of 4AMF-DOTA(Nd) (10 μmol/L) in 10 mmol/L Tris–HCl buffer, pH 8.0, at 25°C were determined.

Luminescence lifetime measurements

The luminescence lifetime of 4AMF-DOTA(Nd) (10 μmol/L) in 10 mmol/L Tris–HCl buffer, pH 8.0, at 25°C was determined. Data were collected at 1 μs resolution and fitted to a single-exponential curve using the equation shown below, where I_0 and I are the luminescence intensities at time $t = 0$ and time t, respectively, and τ is the luminescence emission lifetime. Lifetime was obtained by monitoring emission intensity at 870 nm ($\lambda_{ex} = 488$ nm):

$$I = I_0 \exp(-t/\tau)$$

Synthesis

4-(Chloromethylamido)fluorescein (4AMF-Cl). 4-Aminofluorescein (1.0 g, 3.0 mmol) was dissolved in acetone (20 mL). To the solution was added $ClCH_2COCl$ (372 mg, 3.3 mmol) in acetone solution (10 mL). A yellow powder was formed instantly. The mixture was then stirred for 5 h at room temperature. The mixture was concentrated by evaporation and the resulting residue was redissolved in MeOH. The solution was poured into Et_2O (200 mL), and the resulting residue was washed with Et_2O by decantation three times. The powder was dried under vacuum to obtain 4AMF-Cl (852 mg, 1.9 mmol, 61%) as a yellow powder. MS (ESI, pos.), m/z found 425 ($[M+H]^+$), calcd. 425 ^{1}H-NMR (400 MHz, CD_3OD) δ 8.60 (1H, d, $J = 2.2$ Hz), 8.16 (1H, dd, $J = 2.2$, 8.3 Hz), 7.48 (2H, d, $J = 9.0$ Hz), 7.44 (1H, d, $J = 8.3$ Hz), 7.29 (2H, d, $J = 2.2$ Hz), 7.14 (2H, dd, $J = 2.2$, 9.0 Hz), 4.29 (2H, s).

1-(4-Amidomethyl-fluorescein)-1,4,7,10-tetraazacyclododecane (4AMF-cyclen). A dry DMF suspension (10 mL) of 1,4,7,10-tetraazacyclododecane tetrahydrochloride (cyclen 4HCl) (318 mg, 1.0 mmol), K_2CO_3 (1.4 g, 10.1 mmol) and KI (1.7 g, 10.1 mmol) was stirred for 5 min at 80°C under anaerobic conditions. To the suspension was then slowly added 4AMF-Cl (424 mg, 1.0 mmol) in dry DMF solution (10 mL). After stirring for 9 h at 80°C, the suspension was filtered and the obtained residue was washed with MeCN. The residue was added to MeOH (20 mL). After stirring for 30 min, the reddish suspension was filtered and the obtained residue was washed with MeOH. The filtrate was concentrated by evaporation and the resulting residue was redissolved in a minimum amount of MeOH. The solution was poured into Et_2O (200 mL), and the resulting residue was washed with Et_2O by decantation three times. The powder was dried under vacuum to obtain 4AMF-cyclen (336 mg, 0.6 mmol, 60%) as a red powder. MS (ESI, pos.) m/z found 560 ($[M+H]^+$), calcd. 560. ^{1}H-NMR (400 MHz, DMSO-d_6) δ 8.38 (1H, s), 7.91 (1H, d, $J = 7.3$ Hz), 6.62 (3H, m), 6.52 (2H, s), 6.44 (2H, dd, $J = 1.9$, 8.7 Hz), 3.17 (2H, s), 2.66 (16H, br).

1-(4-Amidomethyl-fluorescein)-1,4,7,10-tetraazacyclododecane-4,7,10-triacetic acid (4AMF-DOTA). To MeOH solution containing 4AMF-cyclen (559.6 mg, 1.0 mmol) and Et_3N (1.4 mL, 10 mmol) was added $BrCH_2COOH$ (556 mg, 4.0 mmol) in MeOH (20 mL) solution at room temperature. The solution was then warmed to 60°C and stirred for 12 h. The mixture was evaporated to remove the solvent. The yellow residue was added to MeOH (20 mL). The suspension was centrifuged (1500 × g, 10 min) and the supernatant was removed. This procedure was repeated five times. The resulting powder was dried under vacuum to obtain 4AMF-DOTA (550.3 mg, 0.8 mmol, 75%) as a yellow powder. MS (ESI, neg.) m/z found 732 ($[M-H]^-$), calcd. 732.

^{1}H-NMR (400 MHz, DMSO-d_6) δ 8.24 (1H, s), 7.68 (1H, s), 6.50–6.70 (7H, m), 4.15 (6H, br), 3.16 (18H, m).

4AMF-DOTA(Nd). To 0.01 mol/L TEAAc buffer, pH 6.5, solution (2 mL) containing 4AMF-DOTA (7.3 mg, 10 μmol) was added $NdCl_3$ $6H_2O$ (4.3 mg, 15 μmol) in 0.01 mol/L TEAAc buffer, pH 6.5, solution (2 mL). After stirring for 1 h at room temperature, the resulting suspension was filtered. The filtrate was introduced into a preconditioned solid phase extraction column (Waters, stationary phase C_{18}) and the buffer and excess lanthanide ion were washed away with distilled water. The chelate was eluted using a 1:4 methanol:water mixture. The solvent was evaporated, and the residue was dried under vacuum to obtain 4AMF-DOTA(Nd) (5.4 mg, 6.2 μmol, 62%) as a yellow powder. MS(ESI, neg.) m/z found 882 ($[M-H]^-$), calcd. 882.

RESULTS AND DISCUSSION

Synthesis of 4AMF-DOTA(Nd)

4AMF-DOTA was synthesized from 4-aminofluorescein in three steps, as shown in Scheme 1. 4AMF-DOTA(Nd)

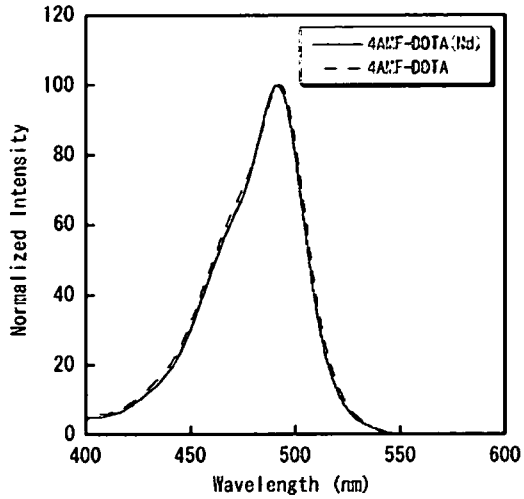

Figure 1. UV-vis absorption spectra of 4AMF-DOTA (dotted line) and 4AMF-DOTA(Nd) (solid line) in 10 mmol/L Tris–HCl buffer, pH 8.0.

was easily synthesized by stirring 4AMF-DOTA and $NdCl_3$ in TEAAc buffer, pH 6.5. Other lanthanide complexes, 4AMF-DOTA(Ln) (Ln = Eu, Tb and Yb), were prepared by the same method as for preparing 4AMF-DOTA(Nd), using $EuCl_3$, $TbCl_3$ and $YbCl_3$.

Spectroscopic characterizations of aqueous solution of 4AMF-DOTA(Nd)

UV-vis spectra of aqueous solutions of 4AMF-DOTA(Nd) and 4AMF-DOTA are shown in Fig. 1. These spectra showed the same features, suggesting that the chelation of DOTA to the Nd ion has no effect on the energy level of the fluorescein moiety.

With IR measurement, absorption of the carbonyl C=O stretching was observed at 1749 cm^{-1} for 4AMF-DOTA and 1724 cm^{-1} for 4AMF-DOTA(Nd), and absorption of the amide N–H bending was found at 1609 cm^{-1} for 4AMF-DOTA and 1587 cm^{-1} for 4AMF-DOTA(Nd) (data not shown). These shifts suggest that the three carbonyl groups and one amide group of the DOTA moiety participated in chelating the Nd ion.

The emission spectra of aqueous solutions of 4AMF-DOTA(Nd) and 4AMF-DOTA are shown in Fig. 2A. Although the long-wavelength tail of fluorescein fluorescence was observed in both compounds, two sharp peaks were detected at 870–900 nm in the spectrum of 4AMF-DOTA(Nd) compared with that of 4AMF-DOTA (Fig. 2A, λ_{ex} = 488 nm). These can be assigned to typical Nd $^4F_{3/2}$ to $^4I_{9/2}$ transition. This excitation wavelength is only slightly injurious to living cells. On the other hand, no fluorescent peak was detected for $NdCl_3$ and Nd-DOTA under the same conditions.

The excitation spectra of aqueous solutions of 4AMF-DOTA(Nd) and 4AMF-DOTA showed much the same features (Fig. 2B, λ_{em} = 870 nm for 4AMF-DOTA(Nd) and 515 nm for 4AMF-DOTA), thus supporting that the 870–900 nm luminescence shown in 4AMF-DOTA(Nd) is derived from the transfer of energy from an excited fluorescein moiety.

These results indicate that 4AMF-DOTA(Nd) can emit NIR fluorescence through its excitation by visible light as expected, but the fluorescence intensity is lower than that from fluorescein. This might occur partly because of the very low triplet yield of excited fluorescein. A simple model for the description of the sensitization process is shown in Fig. 3 (17). Energy transfer from fluorescein to the Nd ion occurs in the triplet state of fluorescein. Moreover, singlet energy transfer has been

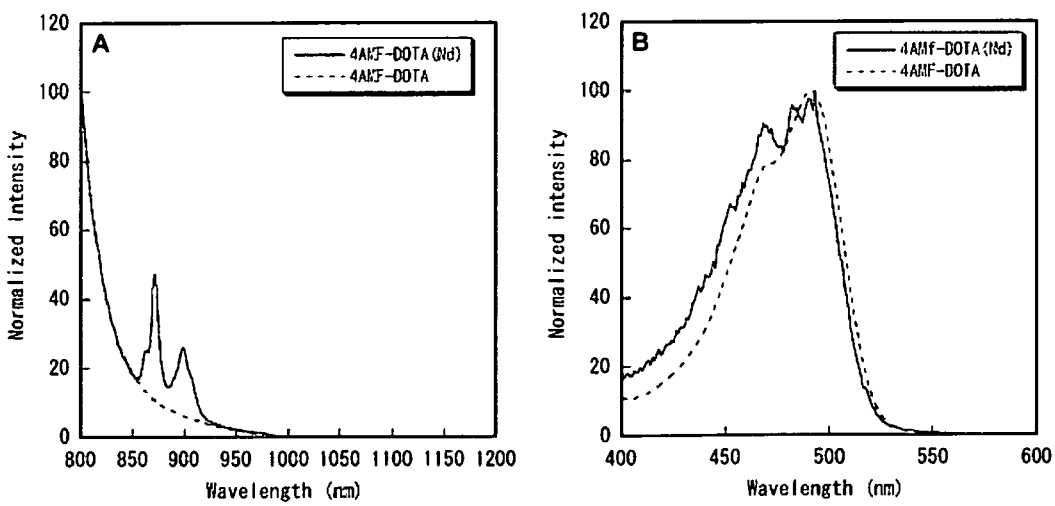

Figure 2. Spectroscopy of 4AMF-DOTA (dotted line) and 4AMF-DOTA(Nd) (solid line) in 10 mmol/L Tris–HCl buffer, pH 8.0. (A) Emission spectra (λ_{ex} = 488 nm). (B) Excitation spectra (λ_{ex} = 870 nm for 4AMF-DOTA(Nd) and 515 nm for 4AMF-DOTA).

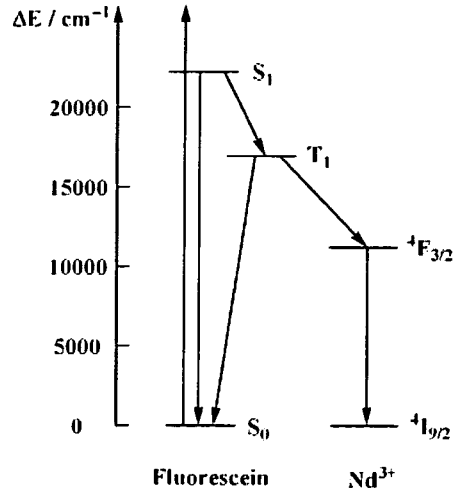

Figure 3. Simple photophysical scheme describing a possible pathway for sensitization of Nd luminescence in 4AMF-DOTA(Nd).

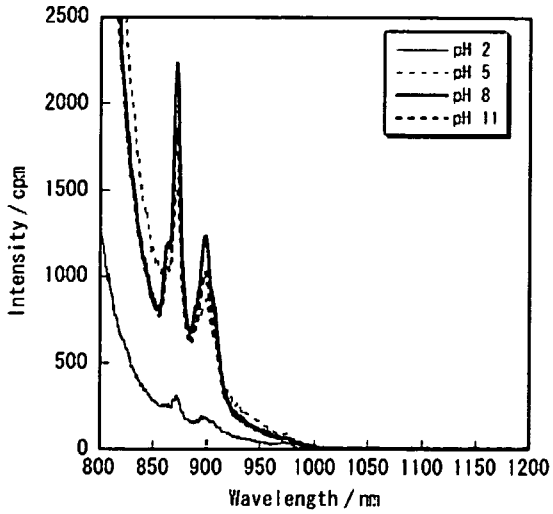

Figure 4. pH effect on the emission spectra of 4AMF-DOTA(Nd) in 10 mmol/L Britton–Robinson buffer.

shown not to contribute significantly to the sensitization process (18).

The energy transfer from the antenna to lanthanide ion has been studied previously (19–21), which has suggested several mechanisms, such as Förster energy transfer (19), Dexter exchange (20) and sequential electronic interaction (21), although none of them has been fully elucidated yet and the mechanism involved in 4AMF-DOTA(Nd) is also unclear. Refining the energy level of fluorescein through derivative syntheses (15) or the use of other chromophores (22, 23) suitable for the Nd ion can be an effective solution.

On the other hand, 4AMF-DOTA(Yb) showed a small peak at approximately 1000 nm due to typical ytterbium $^2F_{5/2}$ to $^2F_{7/2}$ transition, whereas emission peaks of 4AMF-DOTA(Eu) and 4AMF-DOTA(Tb) were not observed, owing to their high excitation levels.

Effects of pH and solvent on the fluorescence of 4AMF-DOTA(Nd)

The effect of pH on the fluorescence of 4AMF-DOTA(Nd) was examined (Fig. 4). The fluorescent intensity of 4AMF-DOTA(Nd) was weak at pH 2, increased with pH and peaked at pH 8. In the pH range 2–11, no degradation product was detected by electrospray mass spectral (ESI–MS) analysis, suggesting the high stability of 4AMF-DOTA(Nd).

It is well known that the fluorescence intensity emitted by fluorescein varies depending on the pH of solvents. The dianionic form of fluorescein in neutral and basic solutions is the most effective to emit fluorescence. In other words, in acidic solution, transition to the ground state of excited fluorescein is carried out without a fluorescent process (24). Therefore, the results shown in Fig. 4 should be regarded as a reflection of the characteristics of fluorescein, supporting the occurrence of energy transfer from fluorescein, the antenna moiety, to the Nd ion.

4AMF-DOTA(Nd) could easily dissolve in many polar organic solvents (e.g. MeOH, EtOH and DMSO). Figure 5 shows the emission spectra (Fig. 5A) and the excitation spectra (Fig. 5B) of 4AMF-DOTA(Nd) in 10 mmol/L Tris–HCl buffer, pH 8.0, and organic solvents such as MeOH, EtOH and DMSO. The λ_{max} of the excitation wavelength against 870 nm emission was 488 nm in aqueous buffer and 498, 504 and 523 nm in MeOH, EtOH and DMSO, respectively (Fig. 5B). On the other hand, the emission spectra showed the same features in the four tested solvents except for intensity at 870 nm and 890 nm (Fig. 5A). This difference in the wavelength shift between excitation and emission spectra may emphasize the orientation of fluorescence, i.e. the results can be considered as follows. In excitation spectra, changes of the λ_{max} in organic solvents are caused by the effect on the energy levels of fluorescein by the solvents, and in the emission spectra the constant wavelength in the four solvents is due to the characteristic of lanthanide ions, that 5s and 5d orbitals are located outside the 4f orbital responsible for fluorescence and protect it from environmental changes. In other words, these data further support that fluorescence around 870–900 nm derives from the Nd ion through energy transfer from the antenna moiety. The emission intensity of 4AMF-DOTA(Nd) shown more strongly in organic solvents than in buffer is probably because H_2O acts as a quencher against excited 4AMF-DOTA(Nd) in some processes.

Long-lived luminescence measurement

Time-resolved fluorescent (TRF) measurement can extract long-lived luminescence. Figure 6 shows the

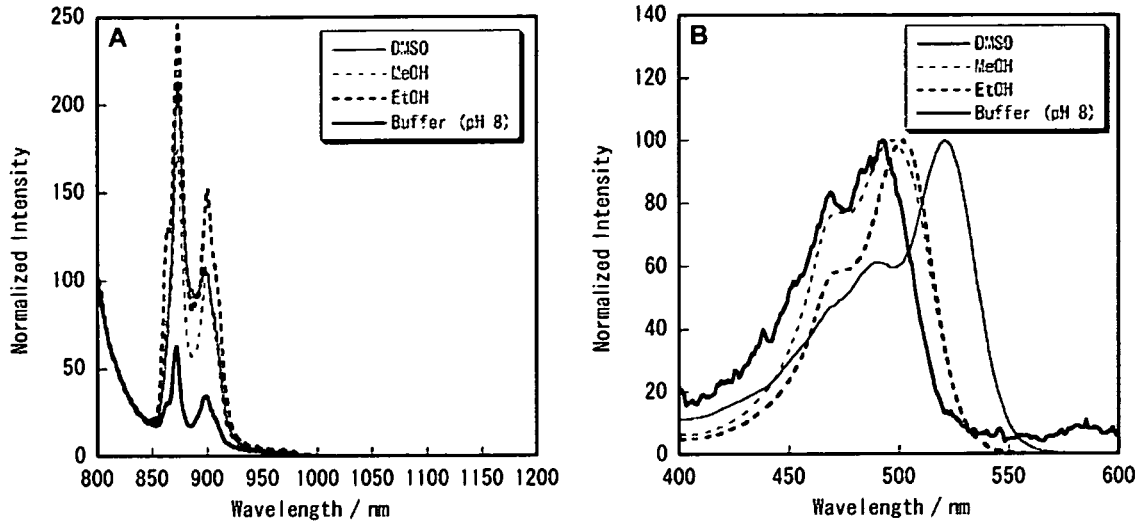

Figure 5. Solvent effect on (A) emission spectra and (B) excitation spectra of 4AMF-DOTA(Nd) in 10 mmol/L Tris–HCl buffer, pH 8.0, MeOH, EtOH and DMSO; each organic solvent contained 0.1% v/v Et_3N.

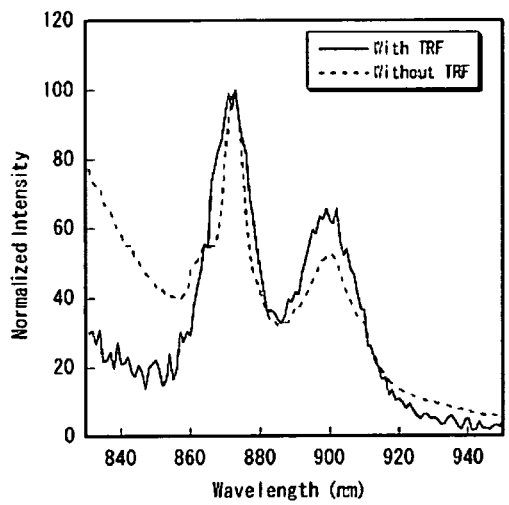

Figure 6. Emission spectra of 4AMF-DOTA(Nd) in 10 mmol/L Tris–HCl buffer, pH 8.0, with (solid line) and without (dotted line) time-resolved measurement.

emission spectra of 4AMF-DOTA(Nd) detected with (solid line) and without (dotted line) TRF measurement. The luminescence of fluorescein and the Nd ion was observed without TRF measurement, as also shown in Fig. 2A, whereas the luminescence of fluorescein disappeared in the detection of emission spectrum with TRF measurement, resulting in the extraction of only Nd luminescence. Furthermore, we calculated the lifetime of Nd ion luminescence using the equation described in the Experimental section. A lifetime of 2.3 μs was consequently obtained as reasonable for a Nd complex, as reported previously (10, 17). In view of the ns-order lifetime of fluorescein [~4 ns (25)], 4AMF-DOTA(Nd) can be considered a potential NIR fluorescent probe able to be detected and imaged separately from fluorescein, scattered or reflected excitation light and other organic fluorophores by the TRF technique.

CONCLUSION

The results obtained in this study indicate that 4AMF-DOTA(Nd) has the potential for *in vivo* fluorescence imaging, with several favourable properties, such as near-infrared luminescence, visible light excitation, long lifetime and large Stoke's shift.

Acknowledgement

This work was partly supported by the Twenty-first Century Center of Excellence Programme 'Knowledge Information Infrastructure for Genome Science'.

REFERENCES

1. Fu G, Yang HY, Wang C, Zhang F, You ZD, Wang GY, He C, Chen YZ, Xu ZZ. Detection of constitutive heterodimerization of the integrin Mac-1 subunits by fluorescence resonance energy transfer in living cells.*Biochem. Biophys. Res. Commun.*2006; **346**: 986.
2. Wandelt B, Cywinski P, Darling GD, Stranix BR. Single cell measurement of micro-viscosity by ratio imaging of fluorescence of styrylpyridinium probe. *Biosens. Bioelectron.* 2005; **20**: 1728.
3. Mizukami S, Kikuchi K, Higuchi T, Urano Y, Mashima T, Tsuruo T, Nagano T. Imaging of caspase-3 activation in HeLa cells stimulated with etoposide using a novel fluorescent probe. *FEBS Lett.* 1999; **453**: 356.
4. Konig K. Multiphoton microscopy in life sciences*J. Microsc.* 2000; **200**: 83.
5. Hansch A, Frey O, Sauner D, Hilger I, Haas M, Malich A, Brauer R, Kaiser WA. *In vivo* imaging of experimental arthritis with near-infrared fluorescence. *Arthrit. Rheum.* 2004; **50**: 961.

6. Chen X, Conti PS, Moats RA. *In vivo* near-infrared fluorescence imaging of integrin $\alpha v\beta 3$ in brain tumor xenografts. *Cancer Res.* 2004; **64**: 8009.
7. Wunder A, Tung CH, Muller-Ladner U, Weissleder R, Mahmood U. *In vivo* imaging of protease activity in arthritis: a novel approach for monitoring treatment response. *Arthrit. Rheum.* 2004; **50**: 2459.
8. Faulkner S, Carrie MC, Pope SJ, Squire J, Beeby A, Sammes PG. Pyrene-sensitized near-IR luminescence from ytterbium and neodymium complexes. *Dalton Trans.* 2004; 1405.
9. Beer PD, Szemes F, Passaniti P, Maestri M. Luminescent ruthenium(II) bipyridine-calix[4]arene complexes as receptors for lanthanide cations. *Inorg. Chem.* 2004; **43**: 3965.
10. Hasegawa Y, Ohkubo T, Sogabe K, Kawamura Y, Wada Y, Nakashima N, Yanagida S. Luminescence of novel neodymium sulfonylaminate complexes in organic media. *Angew. Chem. Int. Ed. Engl.* 2000; **39**: 357.
11. Becker CF, Clayton D, Shapovalov G, Lester HA, Kochendoerfer GG. On-resin assembly of a linkerless lanthanide(III)-based luminescence label and its application to the total synthesis of site-specifically labeled mechanosensitive channels. *Bioconjug. Chem.* 2004; **15**: 1118.
12. Wu SL, Horrocks WD. Direct determination of stability constants of lanthanide ion chelates by laser-excited europium(III) luminescence spectroscopy: application to cyclic and acyclic aminocarboxylate complexes. *J. Chem. Soc. Dalton* 1997; 1497.
13. Quici S, Marzanni G, Forni A, Accorsi G, Barigelletti F. New lanthanide complexes for sensitized visible and near-IR light emission: synthesis, ^{1}H-NMR, and X-ray structural investigation and photophysical properties. *Inorg. Chem.* 2004; **43**: 1294.
14. Werts MHV, Hofstraat JW, Geurts FAJ, Verhoeven JW. Fluorescein and eosin as sensitizing chromophores in near-infrared luminescent ytterbium(III), neodymium(III) and erbium(III) chelates. *Chem. Phys. Lett.* 1997; **276**: 196.
15. Nolan EM, Burdette SC, Harvey JH, Hilderbrand SA, Lippard SJ. Synthesis and characterization of zinc sensors based on a monosubstituted fluorescein platform. *Inorg. Chem.* 2004; **43**: 2624.
16. Brown L, Halling PJ, Johnston GA, Suckling CJ, Valivety RH. The synthesis of some water-insoluble dyes for the measurement of pH in water-immiscible solvents. *J. Chem. Soc. Perk. Trans.* **1**: 1990: 3349.
17. Bassett AP, Magennis SW, Glover PB, Lewis DJ, Spencer N, Parsons S, Williams RM, De Cola L, Pikramenou Z. Highly luminescent, triple- and quadruple-stranded, dinuclear Eu, Nd, and Sm(III) lanthanide complexes based on bis-diketonate ligands. *J. Am. Chem. Soc.* 2004; **126**: 9413.
18. Crosby GA, Alire RM, Whan RE. Intramolecular energy transfer in rare earth chelates – role of triplet state*J. Chem. Phys.* 1961; **34**: 743.
19. Clarkson IM, Beeby A, Bruce JI, Govenlock LJ, Lowe MP, Mathieu CE, Parker D, Senanayake K. Experimental assessment of the efficacy of sensitized emission in water from a europium ion, following intramolecular excitation by a phenanthridinyl group*N. J. Chem.* 2000; **24**: 377.
20. Barigelletti F, Flamigni L, Balzani V, Collin JP, Sauvage JP, Sour A, Constable EC, Thompson AMWC. Intramolecular energy transfer through phenyl bridges in rod-like dinuclear Ru(II)/Os(II) terpyridine-type complexes. *Coord. Chem. Rev.* 1994; **132**: 209.
21. Faulkner S, Burton-Pye BP, Khan T, Martin LR, Wray SD, Skabara PJ. Interaction between tetrathiafulvalene carboxylic acid and ytterbium D03A: solution state self-assembly of a ternary complex which is luminescent in the near IR. *Chem. Commun.* 2002; 1668.
22. Gunnlaugsson T, MacDonaill DA, Parker D. Lanthanide macrocyclic quinolyl conjugates as luminescent molecular-level devices. *J. Am. Chem. Soc.* 2001; **123**: 12866.
23. Quici S, Marzanni G, Cavazzini M, Anelli PL, Botta M, Gianolio E, Accorsi G, Armaroli N, Barigelletti F. Highly luminescent Eu^{3+} and Tb^{3+} macrocyclic complexes bearing an appended phenanthroline chromophore. *Inorg. Chem.* 2002; **41**: 2777.
24. Urano Y, Kamiya M, Kanda K, Ueno T, Hirose K, Nagano T. Evolution of fluorescein as a platform for finely tunable fluorescence probes. *J. Am. Chem. Soc.* 2005; **127**: 4888.
25. Thevenin BJM, Periasamy N, Shohet SB, Verkman AS. Segmental dynamics of the cytoplasmic domain of erythrocyte band 3 determined by time-resolved fluorescence anisotropy – sensitivity to pH and ligand-binding. *Proc. Natl Acad. Sci. USA* 1994; **91**: 1741.